Mapping the bathymetric evolution of the Northern North Sea: from Jurassic synrift archipelago through Cretaceous–Tertiary post-rift subsidence

Alan M. Roberts[1]*, Nick J. Kusznir[1,2], Graham Yielding[1] & Hugh Beeley[3]

[1] Badley Geoscience Ltd, North Beck House, North Beck Lane, Spilsby, Lincolnshire PE23 5NB, UK
[2] Department of Earth & Ocean Sciences, University of Liverpool, Liverpool L69 3BX, UK
[3] ConocoPhillips (UK) Ltd, Rubislaw House, North Anderson Drive, Aberdeen AB15 6FZ, UK
AMR, 0000-0003-4839-0741; GY, 0000-0002-9755-3925; HB, 0000-0003-2919-7137
* Corresponding author: alan@badleys.co.uk

Abstract: The post-rift history of the North Viking Graben has been backstripped in 3D, producing a sequence of palaeobathymetric maps that culminates at the Late Jurassic synrift stage. The backstripping takes into account the three main processes which drive post-rift basin development: thermal subsidence, flexural-isostatic loading and sediment compaction. Before backstripping was performed, the Norwegian Trench, a bathymetric feature within the present-day seabed, was smoothed in order to remove associated decompaction artefacts within the backstripping results.

Palaeobathymetric restorations at the top and base of the Paleocene take into account regional transient dynamic uplift, probably related to the Iceland Plume. 350 m of uplift is incorporated at the Base Tertiary (65 Ma) and 300 m at the Top Balder Formation (54 Ma), followed by rapid collapse of this same uplift.

At the top of the Lower Cretaceous (98.9 Ma), very localized fault-block topography, inherited from the Jurassic rift, is predicted to have remained emergent within the basin. At the Base Cretaceous (140 Ma), the fault-block topography is much more prominent and numerous isolated footwall islands are shown to have been present. At the Late Jurassic synrift stage (155 Ma), these islands are linked to form emergent island chains along the footwalls of all of the major faults. This is the Jurassic archipelago, the islands of which were the products of synrift footwall uplift. The predicted magnitude and distribution of footwall emergence calibrates well against available well data and published stratigraphic information, providing important constraints on the reliability of the results.

The North Viking Graben, within the Northern North Sea (Fig. 1a and b), is one of the world's most comprehensively studied subsurface rift basins, as well as being a hydrocarbon province of global significance. Its importance to our understanding of rift basins has covered many topics and processes, both tectonic/geodynamic and sedimentological/depositional. In terms of tectonics/geodynamics, studies of the North Viking Graben have contributed in many areas, including the following:

- The subsidence history of the basin has allowed testing and corroboration of the first-order predictions of the McKenzie model (McKenzie 1978; Jarvis & McKenzie 1980) for lithospheric stretching and subsidence (e.g. Barr 1987; Giltner 1987; Badley et al. 1988; Marsden et al. 1990; White 1990; Kusznir et al. 1991).
- The internal fault-block structure has provided an understanding of how the crests of tilted fault blocks undergo synrift footwall uplift and interact with sea level (e.g. Yielding 1990; Barr 1991; Roberts & Yielding 1991; Yielding & Roberts 1992; Roberts et al. 1993a; Færseth et al. 1995; Berger & Roberts 1999).
- The constraints of the McKenzie subsidence model have been used to make estimates of the stretching (β) factor across the North Viking Graben, which in turn have been used to constrain 2D-backstripping restorations through time, illustrating palaeobathymetry and palaeostructure (e.g. Roberts et al. 1993b, 1995, 1998; Kusznir et al. 1995).
- Deviations from the basic McKenzie subsidence model have been identified within the details of the post-rift sequence

and have allowed transient dynamic uplift associated with the Iceland Plume to be quantified (e.g. Bertram & Milton 1988; Nadin & Kusznir 1995; Nadin et al. 1995, 1997).

Several further papers of relevance, which follow from this initial work in the 1980s and 1990s, can be found in a Geological Society Special Publication edited by Nøttvedt (2000). In particular, Christiansson et al. (2000), Odinsen et al. (2000a, b) and Ter Voorde et al. (2000) collectively investigated the crustal structure and stretching history of the basin in some detail, revisiting some of the regional seismic lines used in the earlier modelling. Subsequent work on the structure of the North Viking Graben has continued to the present day (e.g. Fazlikhani et al. 2017 and references therein; Fossen et al. 2017).

Figure 2a–c illustrates the background to some of this earlier work with three regional cross-sections. Figure 2a shows a section from Marsden et al. (1990, their Profile-1) and Kusznir et al. (1991), along the deep-seismic line acquired by Britoil in the mid-1980s (Beach et al. 1987). Figure 2b illustrates a section along seismic line NNST-84-10, from Roberts et al. (1993b) and Kusznir et al. (1995). Figure 2c illustrates a section from Christiansson et al. (2000) (also used by Odinsen et al. 2000a, b; Ter Voorde et al. 2000), along deep-seismic line NSDP84-1 (Klemperer & Hobbs 1991; also Profile-2 in Marsden et al. 1990).

Despite this comprehensive body of work, much of it now more than 20 years old, these studies have not yet been complemented by a published 3D restoration history for the North Viking Graben which takes into account all of the main tectonic and geodynamic
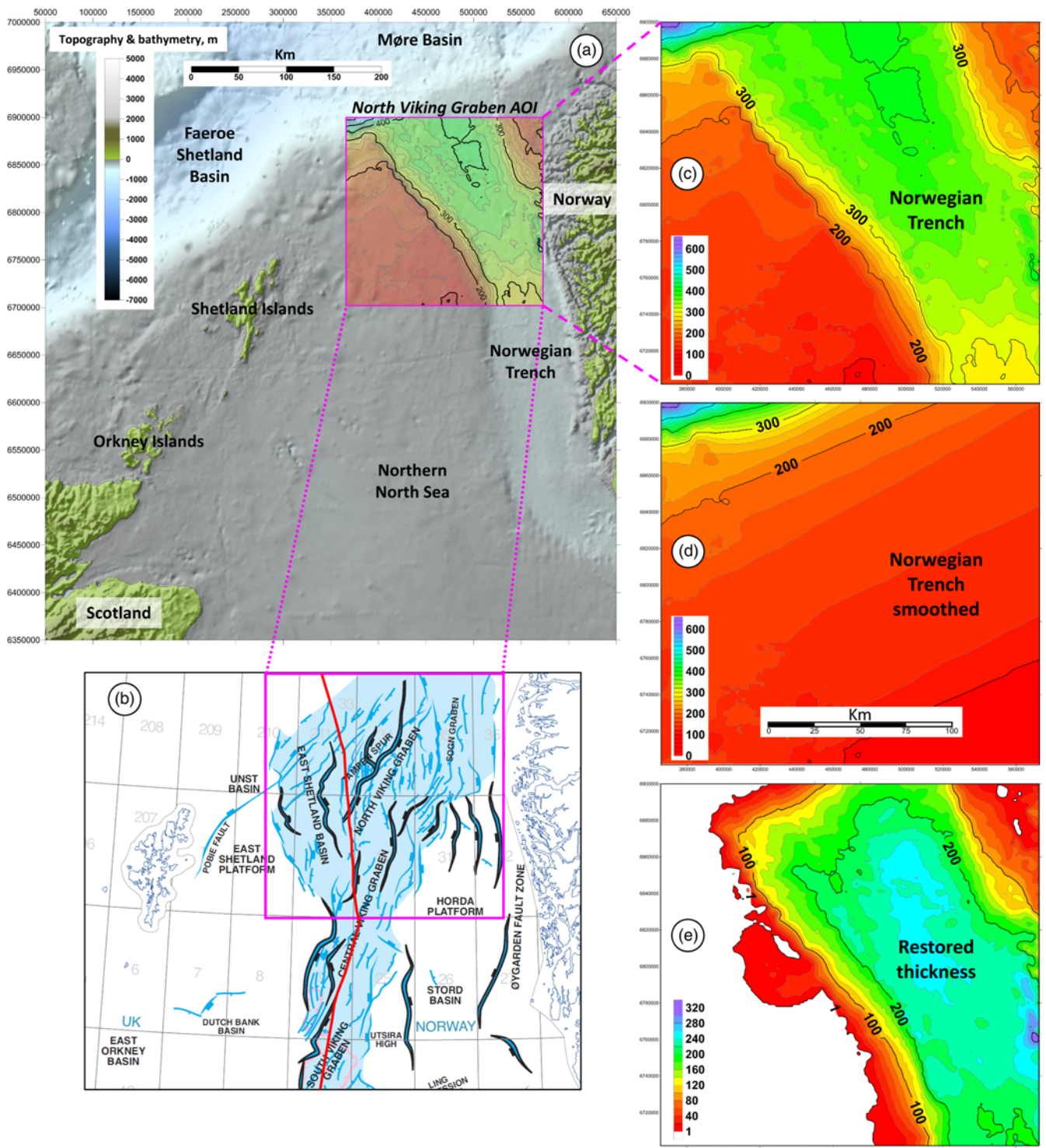
Fig. 1. (**a**) Shaded-relief bathymetry/topography (Smith & Sandwell 1997; scale in metres) for the Northern North Sea, Faeroe Shetland Basin and southernmost Møre Basin. The main study area of interest (AOI) of the North Viking Graben (NVG) is highlighted by an inset map of bathymetry (see also c). All maps in this paper are georeferenced by coordinates (m) within UTM Zone 31N. (**b**) The main Late Jurassic structural elements of the Northern North Sea, locating the NVG (after Zanella & Coward 2003, fig.4.4b). The main study area is in the magenta box. The UK–Norway offshore boundary is shown by a red line. (**c**) Present-day bathymetry of the NVG (see also a), highlighting the Quaternary erosional feature of the Norwegian Trench cutting into a regional background bathymetry of *c*. 100–200 m. (**d**) Smoothed bathymetry for the NVG, in which the Norwegian Trench has been 'filled' by extrapolating the contour trend from the west. (**e**) Thickness of sediment restored by smoothing the seabed. All depths/thicknesses are in metres.

influences identified by the earlier work. This paper, derived from what was initially a commercial study, aims to fill this gap by presenting a sequence of palaeobathymetric maps for the North Viking Graben, produced by application of the established technique of 3D flexural-backstripping and reverse thermal-subsidence modelling (Roberts et al. 2009, 2013, 2018).

Tectonic history of the North Viking Graben

It has been recognized since the 1980s that the basins which comprise the Northern North Sea, including the North Viking Graben, were produced by two episodes of intra-continental rifting, during the Permo-Triassic and Late Jurassic, followed by thermal subsidence through to the present day. The key papers which
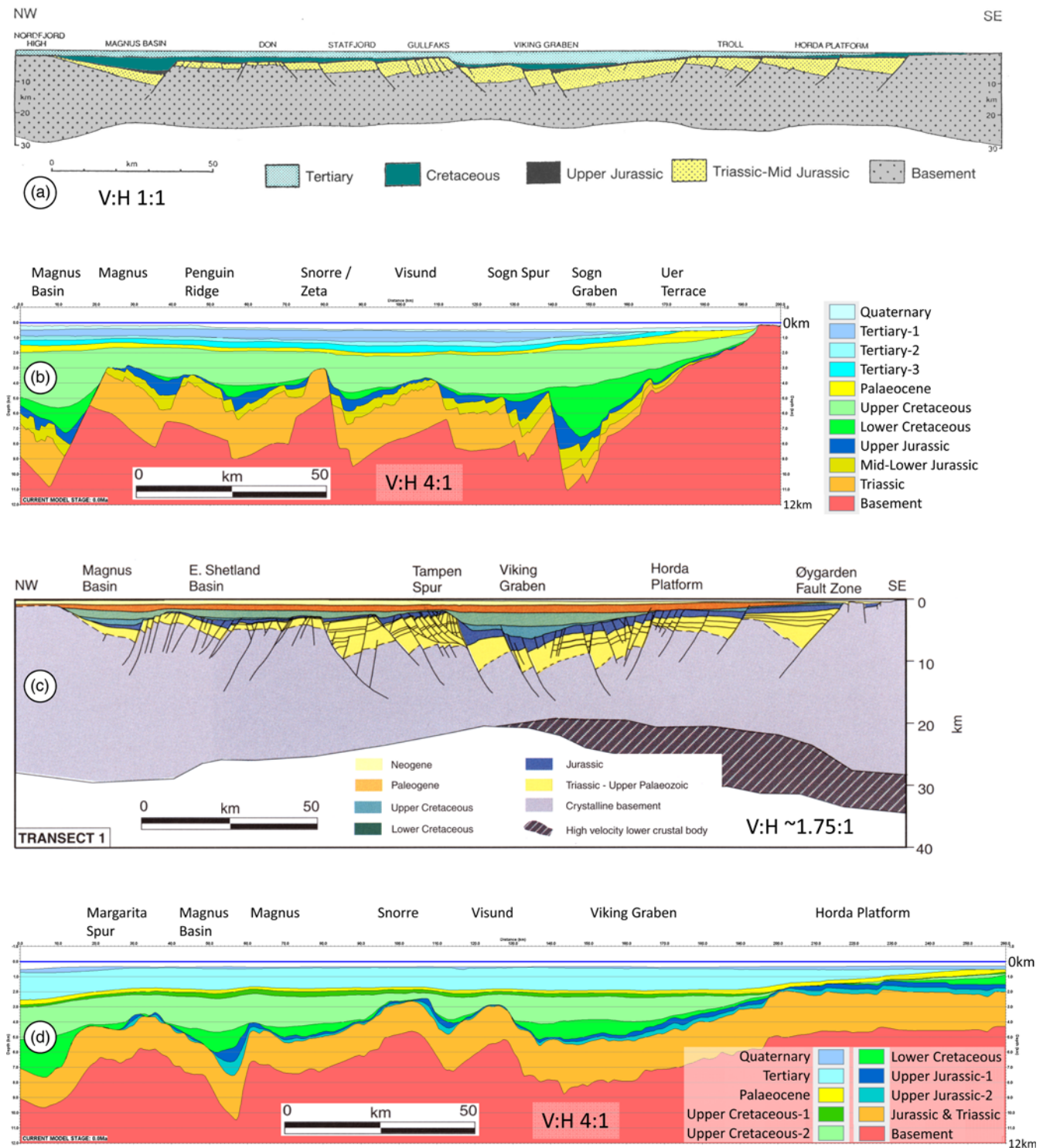
Fig. 2. Four cross-sections used as the basis for quantitative modelling in the Northern Viking Graben. (**a**) Marsden *et al.* 1990, Profile 1, along the Britoil NW–SE deep-seismic profile (Beach *et al.* 1987). (**b**) From Roberts *et al.* (1993*b*) and Kusznir *et al.* (1995), along west–east seismic line NNST-84-10. Reproduced here in colour. (**c**) Christiansson *et al.* 2000, Transect 1, along BIRPS NW–SE deep-seismic profile NSDP84-1 (Klemperer & Hobbs 1991). (**d**) NW–SE cross-section extracted from the grids used in the current study, located in Figure 4b. The seabed is the present-day unsmoothed seabed. V:H, vertical:horizontal.

identified the earlier, deeper Permo-Triassic rift and thus established the two-stage rift history were Eynon (1981) and Badley *et al.* (1984) (see also later work by Steel & Ryseth 1990). Subsequent summaries of the rift history, the conclusions of which remain relevant today, can be found in Badley *et al.* (1988), Yielding *et al.* (1992) and Færseth (1996).

By the early 1990s it had also been recognized that while the overall subsidence history of the Northern North Sea can be described in terms of synrift/post-rift subsidence (McKenzie 1978),

there is a subsidence anomaly within the Paleocene sequence which indicates a period of transient uplift during the Paleocene, followed by a period of accelerated post-Paleocene subsidence (Bertram & Milton 1988; Milton *et al.* 1990; Joy 1992, 1993). This uplift has been quantified across the Northern North Sea as *c.* 300–500 m in magnitude (Milton *et al.* 1990; Nadin & Kusznir 1995; Maclennan & Lovell 2002) and has been ascribed to transient dynamic uplift by the Iceland Plume during the opening of the North Atlantic (Nadin *et al.* 1995, 1997). Transient Early–Middle Jurassic uplift, focused

on the central North Sea (Underhill & Partington 1993a, b), did not extend as far north as the North Viking Graben, although it was significant further south.

In summary therefore, the consensus view of the major tectonic events which led to the formation of the North Viking Graben is as follows:

- intra-continental rifting in the late Permian–early Triassic;
- post-rift thermal subsidence through to the Middle Jurassic;
- a second rift episode in the Late Jurassic;
- thermal subsidence through the Cretaceous;
- transient dynamic uplift during the Paleocene, superimposed on the continued effects of thermal subsidence;
- accelerated subsidence during the Eocene, as a consequence of the withdrawal of dynamic plume support;
- continued thermal subsidence to the present day.

The backstripping model presented in this paper incorporates each of these events.

3D flexural-backstripping and reverse thermal-subsidence modelling

The 3D flexural-backstripping method used in this study was described in detail by Roberts *et al.* (2009), and was itself a development on the 2D flexural-backstripping method described by Kusznir *et al.* (1995) and Roberts *et al.* (1998). The 3D flexural-backstripping method has also been incorporated into the work of Roberts *et al.* (2013, 2018) and Steinberg *et al.* (2018). It is therefore an established technique, well documented in previous literature.

In summary, the method reverse-models the three first-order processes associated with post-rift basin subsidence:

- Thermal subsidence in response to post-rift cooling of the lithosphere. When modelled in reverse, this introduces a thermal uplift back through time. The magnitude of the thermal subsidence is controlled by the β (stretching) factor related to rifting (McKenzie 1978). The backstripping method is able to incorporate the thermal consequences of two rift events: the first of which is described by a constant value of β factor; and the second of which can be described either by a constant value of β factor or, more commonly, by a map of variable β factors.
- Flexural-isostatic subsidence in response to the imposition of sediment loads within the post-rift basin. When modelled in reverse, this leads to flexural-isostatic unloading in response to the progressive removal of the stratigraphic section during backstripping. The form of the flexural-isostatic response is controlled by the effective elastic thickness (T_e) assigned to the model (e.g. Roberts *et al.* 1998).
- Sediment compaction in response to progressive burial. When modelled in reverse, this is known as decompaction and is controlled by assigned lithological parameters (Sclater & Christie 1980).

The backstripping stratigraphic sequence for the North Viking Graben

The stratigraphic sequence used for 3D-backstripping of the North Viking Graben is listed in Table 1. It comprises Seabed plus nine subsurface horizons (in depth), compiled from regional mapping by ConocoPhillips. The mapping is based on regional 2D and 3D seismic interpretation by ConocoPhillips, with depth conversion tied to appropriate well control to ensure accuracy. It was assembled as part of ConocoPhillips' regional exploration strategy in this area. The full stratigraphic sequence incorporated in the backstripping

Table 1. *The full suite of stratigraphic horizons used for backstripping, plus their age and associated bulk lithologies (used to constrain decompaction)*

Horizon No.	Horizon name	Age (Ma)	% sand (interval above horizon)	% shale (interval above horizon)
0	Seabed	0		
1	Base Quaternary	1.8	20	80
2	Top Balder Formation	54	5	95
3	Base Tertiary	65	10	90
4	Intra-Upper Cretaceous	72.4	5	95
5	Top Lower Cretaceous	98.9	5	95
6	Base Cretaceous	140	20	80
7	Intra-Upper Jurassic*	155	20	80
8	Top Middle Jurassic	170	20	80
9	Top Basement[†]	250	50	50

*Interpolated synrift horizon, half-distance between horizons 6 and 8. Broadly equivalent to the top of the Heather Formation (base of the Kimmeridge Clay/Draupne Formation).
[†]Extrapolated as an isochore 2 km below the mapped Top Triassic. The Top Triassic is not included in the backstripping model because of a restriction (up to 10) on the number of horizons which can be included.

can be seen in a cross-section extracted from the ConocoPhillips' depth grids (Fig. 2d).

A map of Seabed within the backstripping area (*c*. 200 × 200 km) is illustrated in Figure 1a and c. Five of the subsurface horizons are illustrated in Figure 3. Backstripped palaeobathymetry for each of these subsurface horizons is presented in the discussion that follows. Each of the horizons in the backstripping model has been mapped directly from seismic interpretation, with the exception of the Intra-Upper Jurassic synrift horizon (Fig. 3e) and the Top Basement.

The Intra-Upper Jurassic is broadly equivalent to the top of the Heather Formation. While it is locally possible to pick a Heather/synrift horizon in many parts of the North Viking Graben, it is not possible to pick this event everywhere. A regional approximation of this horizon has therefore been interpolated at 50% thickness between the regionally consistent Base Cretaceous and Top Middle Jurassic horizons. This interpolation is consistent with information presented in regional stratigraphic summaries of the Upper Jurassic by Ravnås *et al.* (2000) and Fraser *et al.* (2003). The significance of this horizon is that it can be associated directly with the Late Jurassic rift age (see below), whereas the Base Cretaceous and Middle Jurassic each lie *c*. 15 myr either side of this event.

The focus of ConocoPhillips' regional seismic interpretation was on Jurassic-and-younger prospectivity. As a consequence, the deepest horizon mapped was the Top Triassic, which has not itself been included in the backstripping model because of a restriction (up to 10) on the number of horizons which can be included. It is important, however, that decompaction of the Triassic should be incorporated into the backstripping, even if backstripping itself does not extend down to this level. The reasons for this and the pitfalls of not doing so were documented by Roberts *et al.* (1998). Top Basement, at the base of the Triassic, was therefore constructed as an isochore 2 km below the mapped Top Triassic and this horizon was incorporated in the backstripping, allowing for decompaction below the Jurassic (Table 1). We readily acknowledge that this is a simplification of the regional depth to basement and the thickness of the Triassic. A cross-section extracted from the maps used in this study (Fig. 2d) can, however, be compared with the older, seismic-based cross-sections (Fig. 2a–c). This comparison shows that the
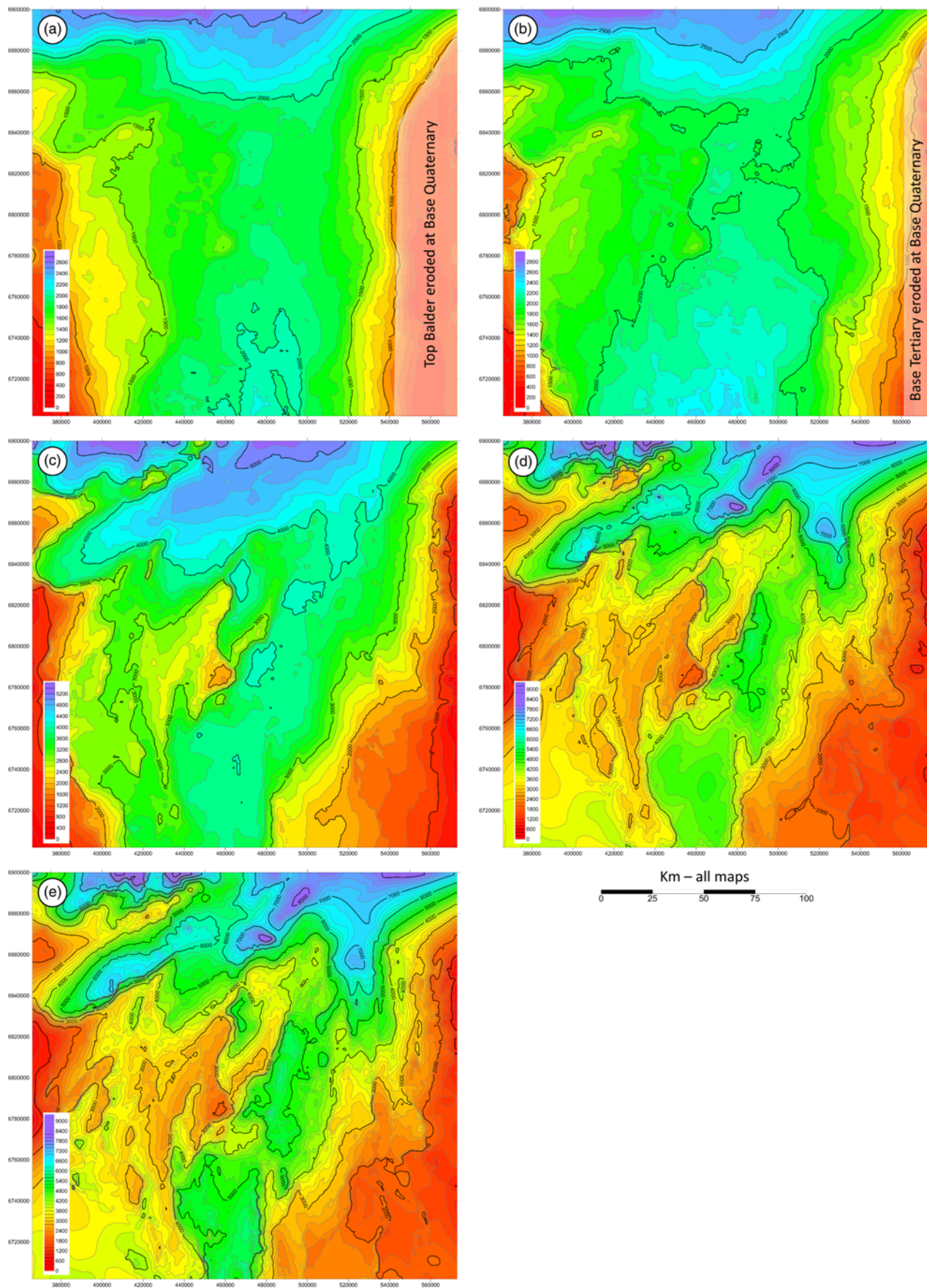
Fig. 3. A selection of the present-day stratigraphic input maps used for backstripping. See Table 1 for the full backstripped stratigraphy. (**a**) Top Balder Formation, 54 Ma. (**b**) Base Tertiary, 65 Ma. (**c**) Top Lower Cretaceous, 98.9 Ma. (**d**) Base Cretaceous, 140 Ma. (**e**) Interpolated Intra-Upper Jurassic synrift, approximating to the Top Heather Formation, 155 Ma. All depths are in metres. In the east the Top Balder and Base Tertiary surfaces are both eroded at the younger Base Quaternary surface. The maps here do not represent the true stratigraphic tops and therefore have a mask placed over them.

extrapolated Top Basement is an acceptable regional approximation, which allows us to mitigate for the absence of a specifically mapped horizon.

Backstripping model parameters for the North Viking Graben

The model parameters used in this study follow from those used by the authors in previous 2D backstripping and forward modelling studies of the North Viking Graben (e.g. Marsden *et al.* 1990; Kusznir *et al.* 1991, 1995; Roberts & Yielding 1991; Roberts *et al.* 1993*b*, 1995, 1998; Nadin & Kusznir 1995). They are also consistent, where appropriate, with those used during 3D backstripping of the Norwegian Atlantic margin immediately to the north (Roberts *et al.* 2009, 2013). This current study uses these previously calibrated parameters as input to a new 3D-backstripping model for the North Viking Graben. The results of this model are then validated against well data from the area in order to ensure that the results themselves can be considered reliable.

Rift ages

The backstripping method implemented here requires instantaneous rift ages (following McKenzie 1978), rather than a time-dependent range (Jarvis & McKenzie 1980). The Permo-Triassic rift is assigned an age of 245 Ma, on the Permian–Triassic boundary (Giltner 1987; Steel & Ryseth 1990; Roberts *et al.* 1995).

The Late Jurassic rift is assigned an age of 155 Ma. It is recognized that this was probably not a geologically instantaneous event and may have progressed throughout much of the Late Jurassic, but an Oxfordian–Kimmeridgian peak (*c*. 155 Ma) is generally accepted (Rattey & Hayward 1993; Roberts *et al.* 1993*a*; Færseth *et al.* 1995; Færseth 1996; Dawers *et al.* 1999) and is an appropriate age for simplification to an instantaneous event.

Magnitude of rifting

The magnitude of rifting, together with the rift age, constrains the magnitude of reverse post-rift thermal subsidence (McKenzie 1978) incorporated into the backstripping.

The backstripping method employed requires the first rift event (of two) to be specified as a constant value of β factor. The Permo-Triassic rift has therefore been assigned an 'average' constant β of 1.25, following the regional forward-modelling analysis by Roberts *et al.* (1995) (see also Færseth 1996). We acknowledge that this may be an underestimate in the area of the graben axis, where the Triassic β factor may rise to *c*. 1.5 (Odinsen *et al.* 2000*b*), but as the Triassic rift (245 Ma) occurred *c*. 90 myr before the Late Jurassic rift (155 Ma), local underestimation of the magnitude of the Triassic rift is not a significant influence on the results when backstripping through the Late Jurassic–present post-rift sequence.

The Late Jurassic rift, more important for the current backstripping, is described by a map of β factors (Fig. 4a). This map is based on the map originally produced by Roberts *et al.* (1993*b*, fig. 8b). The basis on which this map was constructed was a compilation of β profiles from 14 regional seismic lines, produced by forward modelling the Jurassic fault extension on each line (see Roberts *et al.* 1993*b* for further details). The original map has been locally updated and expanded during several subsequent commercial studies, and this updated version is used here (Fig. 4a). The axial region in the centre of the North Viking Graben shows Jurassic β factors of *c*. 1.25. The western flank of the East Shetland Basin and Tampen Spur (Fig. 4b) shows Jurassic β factors of *c*. 1.15, and the eastern flank of the Horda Platform and Uer Terrace shows β factors of *c*. 1.1.

Effective elastic thickness (T_e)

Backstripping has been run using a T_e of 1.5 km controlling the flexural-isostatic response. This is a small, but finite, value which has been calibrated previously and then used successfully for backstripping studies in both the North Viking Graben (Roberts *et al.* 1993*b*, 1998) and on the contiguous Norwegian Atlantic margin to the north (Roberts *et al.* 1997, 2009). Sensitivity tests to the use of other values of T_e have been presented in Roberts *et al.* (1993*b*, 1998) and Kusznir *et al.* (1995) (see also the summary discussion by White 1999). In the backstripping method, T_e is held constant. The value of 1.5 km is, however, calibrated to the synrift/early-post-rift history of the basin (see references above), at which time the stratigraphic loads are short-wavelength (Fig. 2) and the sensitivity to the value of T_e used for backstripping is greatest. During the later post-rift period the stratigraphic loads are long-wavelength (Fig. 2) and there is little sensitivity to the value of T_e used during backstripping; therefore the use of a constant value of T_e throughout the backstripping sequence is not a significant issue (Roberts *et al.* 1998).

Decompaction parameters

Decompaction is performed using the standard layer-based method of Sclater & Christie (1980). The lithology fractions used to constrain the decompaction of each layer are listed in Table 1.

Eustasy

Long-term eustasy is incorporated, using ConocoPhillips' in-house digital formatting of the original data produced by Haq *et al.* (1987).

Previous palaeobathymetric mapping in the North Viking Graben

A small number of previous studies have presented maps of post-rift palaeobathymetry for the North Viking Graben. These maps were the product of 3D-restoration techniques, but were not produced by full 3D-backstripping and reverse thermal-subsidence modelling.

Kjennerud & Sylta (2001) used a purely geometrical approach in their mapping, restoring prograding and deep-marine depositional geometries to produce maps of Tertiary palaeobathymetry for the North Viking Graben. Gabrielsen *et al.* (2001) used decompacted seismic transects in combination with micropalaeontological information to produce maps of Cretaceous palaeobathymetry for the North Viking Graben. There is a solitary claim that 'backstripping methods' were used in this study, but there is no evidence in their subsequent description of methods that any isostatic or thermal calculations were involved in the production of their palaeobathymetry maps. Finally, Kjennerud & Gilmore (2003) used a combination of the previous two methods, restoring depositional geometries in combination with micropalaeontological information, to produce a new set of Tertiary palaeobathymetry maps for the North Viking Graben.

Each of these previous studies incorporated decompaction of the stratigraphy into their approach to 3D restoration, but none of them incorporated the two other first-order contributors to post-rift basin formation: isostasy and thermal subsidence (see the discussion above). This means that in order to produce maps of quantified palaeobathymetry, explicit water-depth markers, either depositional or palaeontological, had to be used in order to datum the maps. The advantage of incorporating the additional processes of isostasy and thermal subsidence, as part of a full backstripping model, is that no explicit water-depth marker or datum is required in order to produce quantified maps. Instead, any information available about water depths or topographical emergence can be used as an independent constraint on the accuracy (and thus reliability) of the backstripping model. The testing of the current backstripping model using
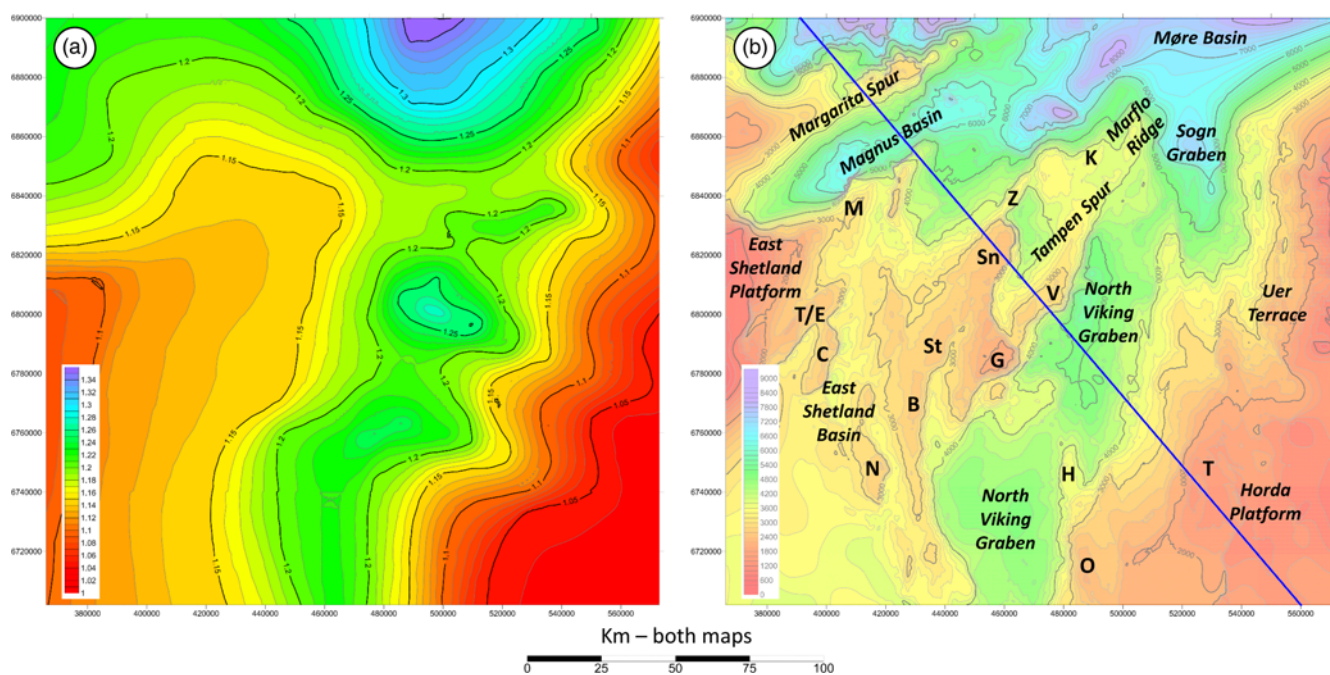
Fig. 4. (**a**) Map of the stretching (*β*) factor for the Late Jurassic rift at 155 Ma, based on Roberts *et al.* (1993*b*, fig. 8b), with subsequent updates. (**b**) Major structural features of the North Viking Graben and significant structural highs coincident with hydrocarbon fields, overlaid on the present-day Base Cretaceous map (Fig. 3d). Hydrocarbon fields: B, Brent; C, Cormorant; G, Gullfaks; H, Huldra; K, Knarr; M, Magnus; N, Ninian; O, Oseberg; Sn, Snorre; St, Statfjord; T, Troll; T/E, Tern/Eider; V, Visund; Z, Zeta Ridge. The blue line is the line of the extracted cross-sections in Figures 2d and 8.

independent constraints from well and seismic data is described in discussion of the results below.

The effect of the Norwegian Trench on backstripping results

In their study of the Norwegian Atlantic margin, Roberts *et al.* (2009) described how the presence of the Storegga Slide at the present-day seabed impacted on backstripping results at all deeper horizons. The Storegga Slide is a large submarine-slide complex which has translated material from the Norwegian coastal shelf towards the Atlantic Ocean to the west. The slide has resulted in a large bathymetric expression on the seafloor and the exhumation of previously buried and partially compacted sediments at the seabed. It is the seabed exposure of these partially compacted sediments which impacts the backstripping. In any backstripping model, the present-day sediment surface is assigned the properties of uncompacted sediment. This causes a problem when erosion/excavation of the seafloor has resulted in the exposure of previously buried sediments, because these sediments then have the wrong compaction condition assigned to them. The result is that a 'decompaction shadow' propagates downwards as an artefact into the backstripping results, as illustrated by Roberts *et al.* (2009, fig. 5). The way to remove this shadow is to fill in the eroded seabed topography, by producing a map of restored seabed (Roberts *et al.* 2009, fig. 6). This has the effect of setting the compaction condition of the 'reburied' sediments to their correct value and the 'decompaction shadow' is removed. All of the best-case results in Roberts *et al.* (2009) were presented from a model in which the Storegga Slide had been restored.

When the first-pass 3D-backstripping of the North Viking Graben was performed as part of the current study a similar 'decompaction shadow' was found in backstripping results below the Norwegian Trench. The Norwegian Trench is a bathymetric feature in the present-day seabed (Fig. 1a and c) within which glacial erosion into the underlying Quaternary sequence has occurred. The trench is located offshore from the Norwegian coast. The 'decompaction shadow' was seen in all backstripped

maps and was particularly obvious below the steeper contours of the SW margin of the trench. The decision was therefore taken to fill in the trench by producing a map of restored seabed and then to use the restored seabed as input to all subsequent backstripping models.

The map of restored seabed is shown in Figure 1d. It was produced by extrapolating the seabed contour pattern from SW of the trench towards the NE and across the trench. The thickness of material restored in this way is shown in Figure 1e. The typical thickness of restored material in the trench is *c*. 200–250 m, reaching a local maximum of *c*. 320 m. The restored seabed (Fig. 1d) was used as the initial model surface for the backstripping model and all associated results presented below, which, as a consequence, show no 'decompaction shadow' below the trench.

It is important to note that while the decompaction issue associated with seabed erosion has been identified specifically in the 3D-backstripping work presented here and by Roberts *et al.* (2009), it will affect any backstripping model, 1D, 2D or 3D, performed in an area of active seabed erosion. It is simply easier to identify the consequences and correct for them when working with maps in 3D rather than when working in 1D or 2D, where the effects are generally less obvious.

Backstripping to the Base Tertiary: acknowledging transient Paleocene uplift

Top Balder Formation (54 Ma)

The first stage of the backstripping sequence for the North Viking Graben covers restoration from the present-day back to the Base Tertiary–Top Cretaceous (65 Ma), taking into account transient Paleocene uplift considered to be related to the Iceland Plume (Bertram & Milton 1988; Milton *et al.* 1990; Nadin & Kusznir 1995; Maclennan & Lovell 2002). To accommodate transient uplift, we have used the method first established in 2D and applied in the North Sea by Nadin & Kusznir (1995) and Nadin *et al.* (1995, 1997). The 2D method has also been used on the Norwegian margin by Roberts *et al.* (1997) and Kusznir *et al.* (2004, 2005). It was first
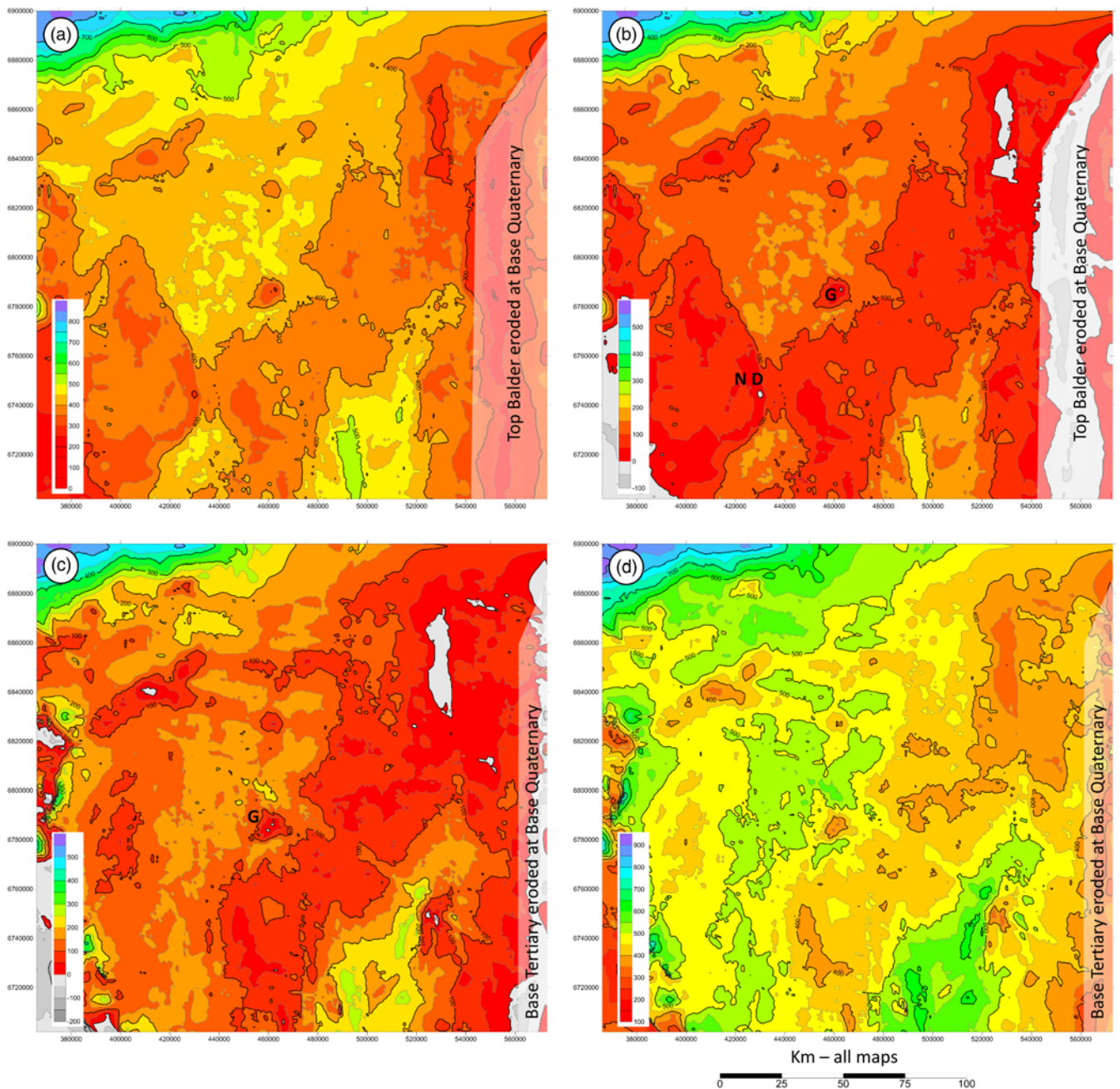
Fig. 5. (a) Backstripped palaeobathymetry at Top Balder (54 Ma), with no transient dynamic uplift. **(b)** Backstripped palaeobathymetry at Top Balder (54 Ma), with 300 m of transient dynamic uplift. G, Gullfaks; ND, Ninian Delta. **(c)** Backstripped palaeobathymetry at Base Tertiary (65 Ma), with 350 m of transient dynamic uplift. **(d)** Backstripped palaeobathymetry at Base Tertiary (65 Ma), with no transient dynamic uplift. All depths are in metres.

applied in 3D, also on the Norwegian margin, by Roberts *et al.* (2009); Figure 5a shows a map of backstripped Top Balder palaeobathymetry (at 54 Ma) for the North Viking Graben. This map has been produced acknowledging the thermal subsidence consequences of the Jurassic and Triassic rift events, but with no transient dynamic uplift incorporated. It is therefore the basic backstripping result. Palaeobathymetry in the central, axial region is typically in the range 350–450 m, becoming slightly shallower on the flanks. Within the context of transient Paleocene uplift, this map represents palaeobathymetry after withdrawal of dynamic plume support, which in the models of Nadin & Kusznir (1995) and Nadin *et al.* (1995, 1997) occurred rapidly in the Eocene.

Figure 5b shows a map of Top Balder palaeobathymetry (54 Ma) produced by incorporating a uniform uplift of 300 m into the result shown in Figure 5a. In all areas mapped as submerged (coloured shading), this is a 300 m direct shift and reduction of bathymetry,

but in the few locally emergent areas (grey shading) isostatic compensation for water-to-air loading is incorporated. The amount of uplift applied has been constrained at 300 m by two features labelled on the map, the crest of the Gullfaks structure (G) and the front of the Ninian Delta (ND) (Bertram & Milton 1988), both of which have been restored locally to sea level.

The Ninian Delta is associated with the local development of Paleocene coals, within a shallow-water deltaic sequence prograding eastwards into the basin from the Shetland Platform to the west. It has long been known to be a palaeosea-level marker on the western side of the North Viking Graben (Bertram & Milton 1988). The Ninian Delta was the primary Paleocene bathymetric marker used by Nadin & Kusznir (1995) and Nadin *et al.* (1995, 1997) in their backstripping of the North Viking Graben. It is therefore appropriate that the front of the delta should be restored to sea level within the 3D-backstripping sequence (Fig. 5b).

The crest of the Gullfaks structure is also restored to sea level by incorporating 300 m of uplift. On the Gullfaks structure, the lithology of the Paleocene sequence is regionally anomalous. Drilling results have shown that it contains shallow-water limestones, unknown elsewhere in the Paleocene of the North Viking Graben (Wennberg *et al.* 2018; see also Statoil 2013, 2015*a*, *b*). This information was not available to previous published backstripping studies in the area, but is compatible with the restoration of the crest of Gullfaks back to, or close to, sea level during the Paleocene as an isolated island or atoll within a shallow-marine sea (Fig. 5b).

The twin constraints of the Ninian Delta and Gullfaks provide good calibration of the transient uplift present at the end of the Paleocene (54 Ma) to be *c.* 300 m. This is slightly lower than the estimate obtained by Nadin & Kusznir (1995) and Nadin *et al.* (1995, 1997), but their work in the North Viking Graben was based on a single regional seismic line and not on a regional 3D stratigraphic model in which all available locations are sampled.

Base Tertiary–Top Cretaceous (65 Ma)

Next in the sequence, Figure 5c shows a map of Base Tertiary (65 Ma) palaeobathymetry, produced by backstripping the model in Figure 5b through a further 11 myr and incorporating 350 m of uplift (50 m more than the 300 m incorporated at the Top Balder). The magnitude of uplift is again calibrated by restoring the crest of the Gullfaks structure to sea level (Statoil 2013, 2015*a*, *b*; Wennberg *et al.* 2018). The Ninian Delta had not yet developed at this stage. Away from any local structural highs, bathymetry at this time is predicted to have been *c.* 50–150 m. Within the context of transient Paleocene uplift, Figure 5c represents palaeobathymetry at the onset of the period of uplift, while Figure 5b represents palaeobathymetry at the end of the period of uplift.

The final map in the Tertiary sequence (Fig. 5d) shows the predicted Base Tertiary (65 Ma) palaeobathymetry after the removal of 350 m of uplift from Figure 5c. It is a return to the basic backstripping result with respect to the two earlier rift events but without any transient uplift. Within the context of transient Paleocene uplift, Figure 5d represents palaeobathymetry at the end of the Cretaceous (regionally *c.* 500 m), immediately prior to the introduction of transient, plume-related uplift. From this point in time, back to the Jurassic, backstripping continues without further need to address external dynamic effects not incorporated into the basic backstripping method.

In the forward sense, a summary of the transient uplift incorporated into the backstripping model is: (i) the introduction of uplift (350 m) at the end of the Cretaceous (65 Ma); (ii) a decrease in the magnitude of uplift to 300 m at the Top Balder (54 Ma); and (iii) collapse of all uplift early in the Eocene.

Backstripping to the Late Jurassic: the synrift archipelago

Results from the second stage of backstripping, from the Base Tertiary (65 Ma) to the Late Jurassic synrift (155 Ma), are shown in Figures 6–8.

Top Lower Cretaceous (98.9 Ma)

Figure 6a shows a map of backstripped Top Lower Cretaceous palaeobathymetry (at 98.9 Ma) for the North Viking Graben. This map has been produced by backstripping a further 33.9 myr from the Top Cretaceous stage of Figure 5d. Figure 7a shows an illuminated 3D perspective display of the same map. Figure 8a shows a cross-section extracted from the model results at this stage,

the present-day version of which is shown in Figure 2d (located in Fig. 4b).

By the time of restoration to the Top Lower Cretaceous, the underlying fault-block topography, developed during the Late Jurassic rift event, has started to become apparent within the regional palaeobathymetry. This is because the basin was significantly sediment-starved throughout the Late Jurassic and Early Cretaceous (Bertram & Milton 1988; Roberts *et al.* 1993*a*), such that the fault-block topography was not fully buried at seabed until the Late Cretaceous. Key to the calibration and reliability of this map is the prediction that the crest of the Gullfaks structure (located in Figs 4b, 5b and 6a) was emergent as an isolated island at this time (grey shading). Emergence of Gullfaks is compatible with the known stratigraphy on the structure, where Fossen & Hesthammer (1998) reported 'A major time gap (up to 100 Ma) is represented by the base Cretaceous (late Cimmerian) unconformity on the Gullfaks Field, separating Upper Cretaceous sediments from Jurassic or Triassic sediments' (p. 233), i.e. Upper Cretaceous is the oldest post-rift cover on the structural crest of Gullfaks; Lower Cretaceous is absent, as predicted by the presence of the emergent island in Figures 6a and 7a.

The other structural feature predicted as emergent in the Top Lower Cretaceous map (Figs 6a and 7a) is the NE part of the Margarita Spur (located in Fig. 4b). Emergence of the NE Margarita Spur at the end of the Early Cretaceous is supported by the stratigraphic sequence in Norwegian well 6201/11-1, located on the crest of the structure (Fig. 6d), which shows Upper Cretaceous post-rift sediments unconformable upon Triassic pre-rift, no Lower Cretaceous or Jurassic is present (NPD Fact Pages for well 6201/11-1: NPD 2018).

The Oseberg structure (Badley *et al.* 1984), situated in the south of study area (Fig. 4b), is not predicted by backstripping to be emergent at the Top Lower Cretaceous but its crest is restored to within <100 m of sea level at this time (Fig. 6a). Oseberg well 30/6-1 shows Upper Cretaceous unconformable on the Heather Formation and well 30/6-2 shows Upper Cretaceous on eroded Middle Jurassic (NPD Fact Pages for wells 30/6-1 and 30/6-2: NPD 2018); both are crestal wells (Fig. 6d). There is no Lower Cretaceous or Upper Jurassic Draupne Formation in either well. The stratigraphic sequence at the crest of Oseberg is therefore compatible with emergence at the top of the Lower Cretaceous or, as predicted by the backstripping, still sitting sufficiently close to sea level that no Lower Cretaceous deposition occurred.

To the best of our knowledge and as predicted by the palaeobathymetric map (Figs 6a and 7a), all other structural highs in the North Viking Graben are capped by a Lower Cretaceous sequence, commonly highly condensed and deposited in a marine setting. Away from the major structural highs, the regional Top Lower Cretaceous bathymetry is in the range *c.* 500–1000 m, although it exceeds 1000 m in the NW of the area around the Margarita Spur (Fig. 8a) and approaching the Møre Basin (Fig. 1a).

Base Cretaceous (140 Ma)

Figure 6b shows a map of backstripped Base Cretaceous palaeobathymetry (at 140 Ma) for the North Viking Graben. This map has been produced by backstripping a further 41.1 myr from the Top Lower Cretaceous stage of Figure 6a. Figure 7b shows an illuminated 3D perspective display of the same map. Figure 8b shows a cross-section extracted from the model results at this stage.

The key feature of the palaeobathymetric map is that it shows a late stage of the emergent synrift archipelago (grey shading) as a scattered set of islands located on fault-block crests. Calibration of this predicted emergence (residual footwall uplift) at the Base Cretaceous ideally requires the Late Jurassic synrift Kimmeridge
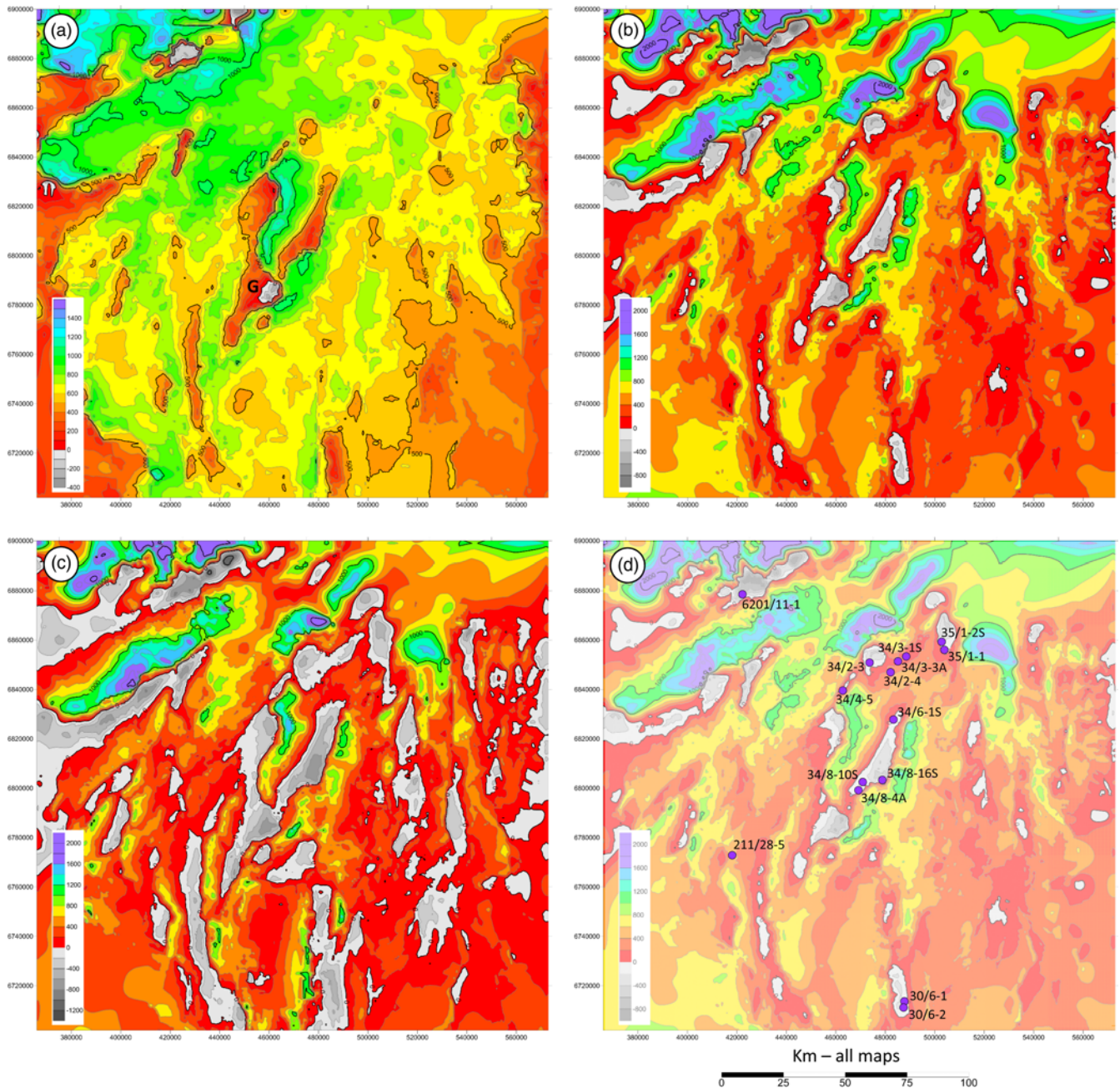
Fig. 6. (**a**) Backstripped palaeobathymetry at Top Lower Cretaceous (98.9 Ma); note the local emergence at the crest of Gullfaks (G). (**b**) Backstripped palaeobathymetry/topography at Base Cretaceous (140 Ma). Elements of the island archipelago remain. (**c**) Backstripped palaeobathymetry/topography at the Late Jurassic synrift (155 Ma). The emergent island archipelago is at its maximum size. All depths/heights are in metres. Grey denotes predicted emergence. (**d**) Wells referred to in the text, overlaid on Base Cretaceous palaeobathymetry (**b** above).

Clay/Draupne (UK/Norway) Formation to be absent and for Cretaceous post-rift sediments to be sitting unconformably on the pre-rift stratigraphy of the Heather Formation or older (Brent Group, Dunlin Group, Triassic). The Heather Formation does itself show evidence of early synrift stratigraphic geometries within many fault blocks, but Rattey & Hayward (1993), Roberts *et al.* (1993*a*), Færseth *et al.* (1995) and Dawers *et al.* (1999) have documented that deposition of the Heather Formation still predated the peak of Late Jurassic fault activity and is on some structures eroded as a consequence of footwall uplift during later Jurassic extension. There are several structures, emergent or very close to sea level within Figure 6b, on which this stratigraphic calibration has been documented and through which the map has been validated. Each of these structures, described below, is located in Figure 4b.

Gullfaks, the Margarita Spur and Oseberg

The emergence of Gullfaks and the Margarita Spur, plus the near-emergence of Oseberg, not just at the Base Cretaceous but onwards to the Top Lower Cretaceous, has been documented above.

Snorre

This is one of the classic eroded fault-block structures in the North Viking Graben and the subject of early quantitative investigations into footwall uplift (Yielding 1990; Yielding & Roberts 1992; Yielding *et al.* 1992). The crest of Snorre has no Jurassic stratigraphy present, but shows condensed Lower Cretaceous post-rift resting unconformably on eroded Triassic pre-rift (Hollander 1987). This is fully compatible with the predictions of Figure 6b.
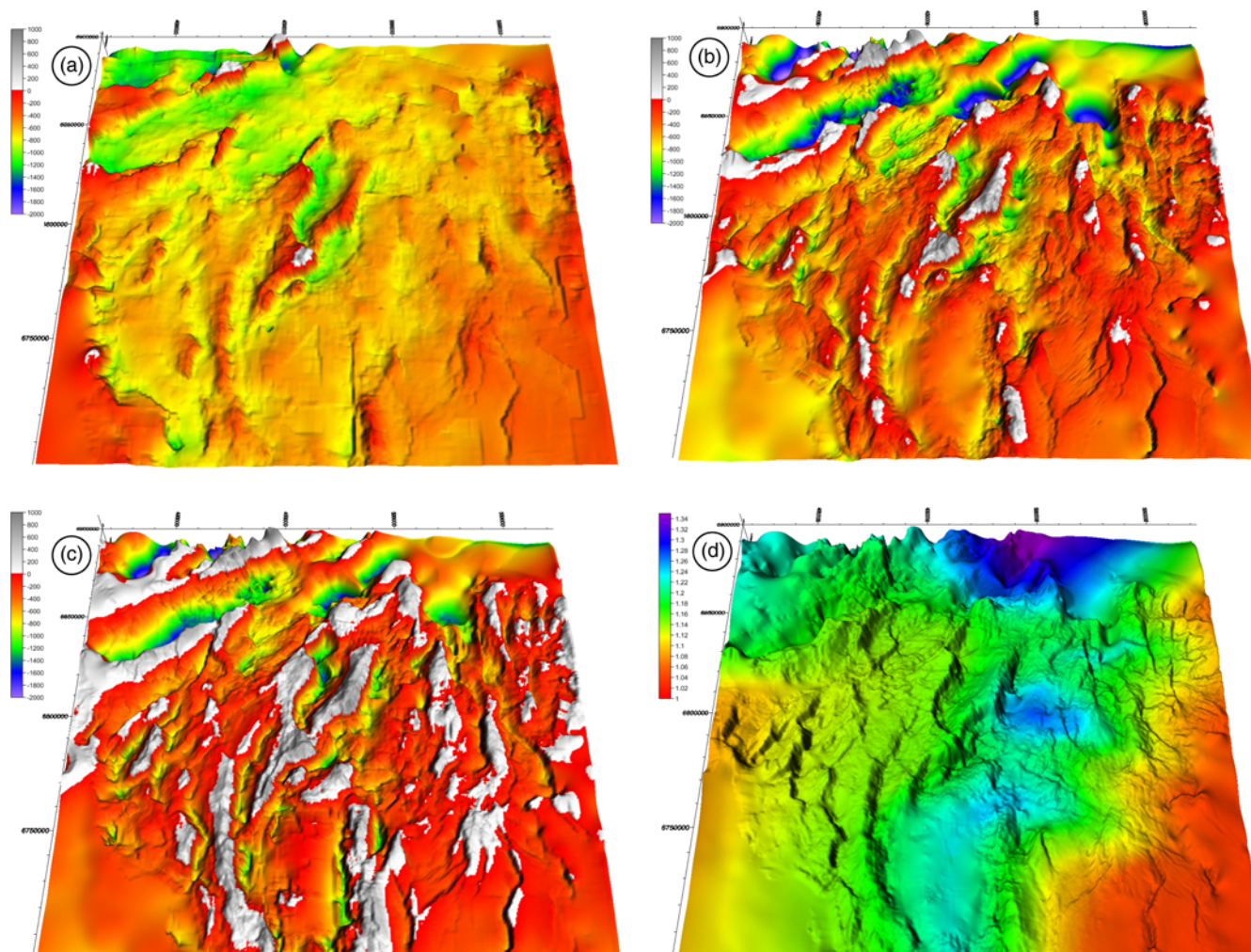
Fig. 7. Illuminated 3D perspective displays (with 7.5:1 vertical exaggeration) of: (**a**) backstripped palaeobathymetry at Top Lower Cretaceous (98.9 Ma: Fig. 6a); (**b**) backstripped palaeobathymetry/topography at Base Cretaceous (140 Ma: Fig. 6b); and (**c**) backstripped palaeobathymetry/topography at the Late Jurassic synrift (155 Ma, Fig. 6c). All depths/heights are in metres. Grey denotes predicted emergence. (**d**) Colour-coded Jurassic β factor (Fig. 4b) displayed on the backstripped topography of the Base Cretaceous (b above). The relationship between the β factor and rift structure can be seen in this display.

Furthermore, the predicted shoreline around Snorre (colour/grey boundary) is coincident with the location of a fringe of Munin Formation Upper Jurassic shallow-marine synrift sandstones on the dip slope of the fault block (Yielding & Roberts 1992, fig. 13; Dahl & Solli 1993, fig. 9).

Visund

Visund is a major fault-block structure located close to both Snorre and Gullfaks. Færseth *et al.* (1995, fig. 9) documented the general absence of an Upper Jurassic sequence on the crest of Visund, the exception being the uppermost Draupne (Ryazanian in age) described as 'condensed section or no deposition'. In more detail, crestal wells 34/8-4A, 34/8-10S and 34/8-16S (Fig. 6d) record Lower Cretaceous resting unconformably on Lower Jurassic, Middle Jurassic and Triassic, respectively, with no Upper Jurassic present (see the NPD Fact Pages for these wells: NPD 2018).

Zeta Ridge

This is a narrow horst north of the Snorre fault block (Fig. 2b). In well 34/4-5, on the crest of the horst (Fig. 6d), a condensed Lower Cretaceous sequence sits unconformably on Middle Jurassic within a synrift degradational fault block (Berger & Roberts 1999); no Draupne Formation is present.

Marflo Ridge and Knarr

This area comprises the northern part of the Tampen Spur, north of Snorre and Visund. There are several wells in this area in which Lower Cretaceous sits unconformably on the pre-rift sequence, with the Draupne Formation absent. From west to east, as examples (Fig. 6d), well 34/2-3 shows Lower Cretaceous on Triassic, well 34/2-4 shows Lower Cretaceous on the Heather Formation, wells 34/3-3A and 34/3-1S show Lower Cretaceous on Lower Jurassic, and wells 35/1-2S and 35/1-1 show Lower Cretaceous on the Heather Formation (see the NPD Fact Pages for these wells: NPD 2018). This area did, in fact, provide the first ever published illustration of palaeobathymetric results from the 3D flexural-backstripping method (Ohm *et al.* 2006, fig. 21, the work for which was performed by two of the current authors, AMR & HB). This previous study was focused specifically on the northern part of the Tampen Spur and was followed later by the more regional study described in this paper. The results of these two studies are fully compatible with each other.

Magnus

The reservoir in the Magnus Field is Upper Jurassic synrift sandstones (Intra-Kimmeridge Clay) on the dip slope of the major Magnus fault block (Figs 2d and 8b). As recorded by Shepherd (1991), however, 'at the crest of the fault-block the Upper
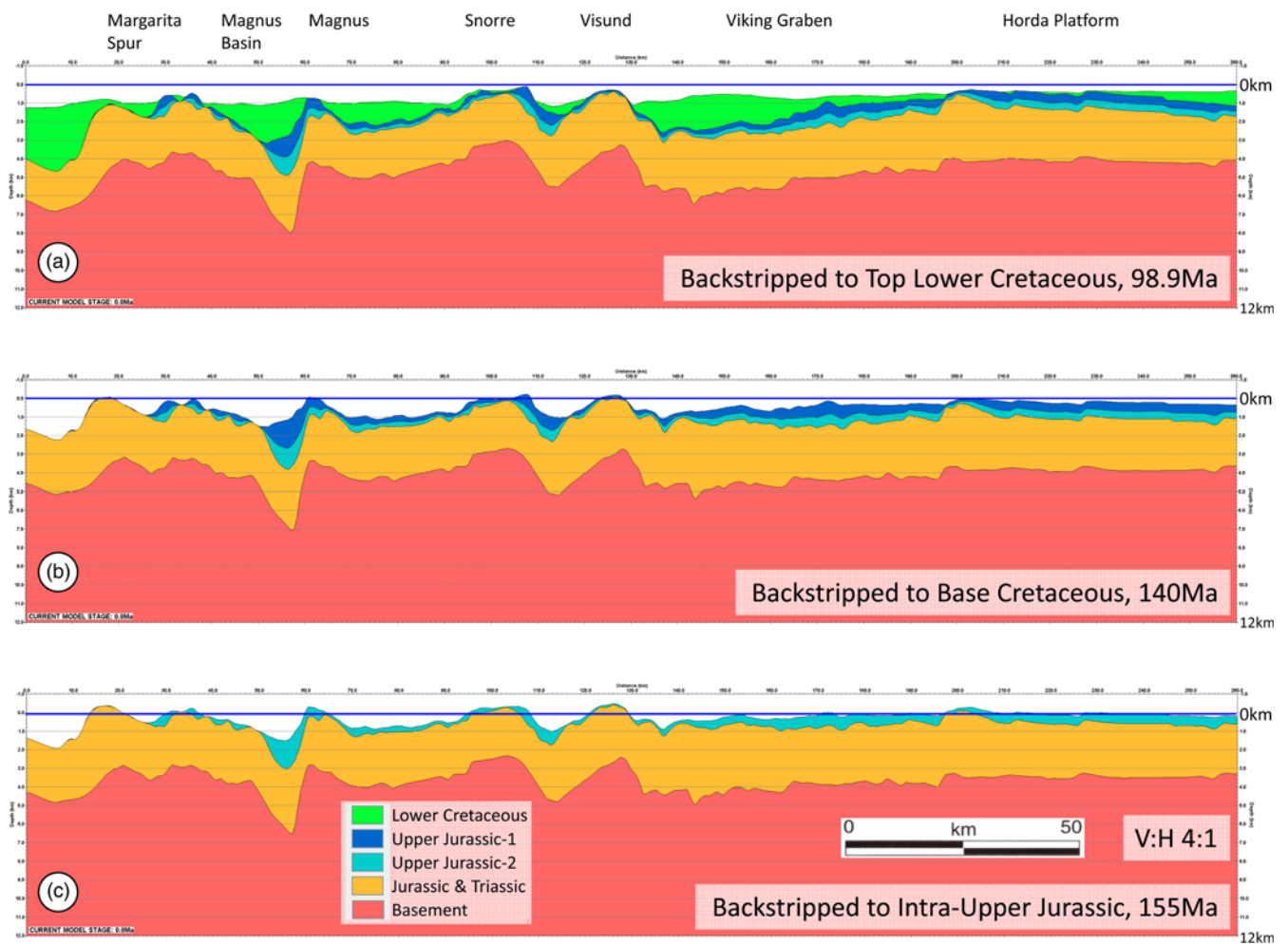
Fig. 8. Three backstripped cross-sections extracted from the 3D results of the current study. The original, present-day section is Figure 2d, located in Figure 4b. (**a**) Backstripped to Top Lower Cretaceous (Figs 6a and 7a). All structural highs on the section are below sea level. (**b**) Backstripped to Base Cretaceous (Figs 6b and 7b). Several structural highs are restored to, or just above, sea level. (**c**) Backstripped to Intra-Upper Jurassic synrift (Figs 6c and 7c). Several structural highs are emergent footwall islands with crests above sea level.

Kimmeridge Clay is absent due to erosion and the vertical seal is provided by Cretaceous mudstones' (Shepherd 1991, figs 2 and 4). Additionally, both the Magnus fault block and the Margarita Spur to the NW have been illustrated as significantly emergent at the Base Cretaceous by Young (1992, fig. 10).

There are thus several examples of structures on which the backstripping predictions of emergence at the Base Cretaceous can be validated. It is also important that structures predicted to be submerged at the Base Cretaceous should be capped by at least the upper (younger) part of the Kimmeridge Clay/Draupne Formation. Structures on which this can be documented, because their crestal synrift degradational complexes are capped by Kimmeridge Clay/ Draupne Formation, are the adjacent Statfjord and Brent fields (Livera & Gdula 1990; Roberts *et al.* 1993*a*; Hesthammer *et al.* 1999), and the Ninian Field (Underhill *et al.* 1997); each are located in Figure 4b.

Away from the focus on the main uplifted and elevated areas within the Base Cretaceous basin, the backstripping also predicts significant water depths within some of the major half-graben structures. In the hanging walls (east) of Snorre, Visund and Gullfaks, bathymetry is locally mapped at >1000 m, while further to the north, approaching the Møre Basin, the predicted bathymetry in places exceeds 1500 m. These bathymetries persist from the Late Jurassic rift episode because the basin was significantly underfilled by the Kimmeridge Clay/Draupne Formation during the latter part of the Late Jurassic.

The Base Cretaceous stratigraphic surface in the North Viking Graben is commonly referred to in the literature and in conversation as the Base Cretaceous Unconformity (or BCU). As first pointed out by Bertram & Milton (1988) and then by Rattey & Hayward (1993), this is not a correct description of the regional nature of this surface. Figures 6b, 7b and 8b show that only at the crests of the largest fault blocks, preferentially drilled by commercial wells, was the Base Cretaceous actually an emergent and eroding surface. Away from the crests of the largest fault blocks the Base Cretaceous was a submarine surface and potentially the site of continuous deposition from the Late Jurassic into the Early Cretaceous. This sequence of continuous deposition has been recorded in the few structurally deep hanging-wall wells drilled within the basin (e.g. well 211/28-5: Fig. 6d), whose downdip location on the Brent fault block is illustrated by Yielding *et al.* (1992, fig. 4).

While Figure 7b shows the illuminated perspective view of Base Cretaceous palaeobathymetry/topography, colour-coded for water depth and emergence, Figure 7d shows the same 3D display of Base Cretaceous structural relief but this time colour-coded to illustrate the map of β factors used to constrain the backstripping (Fig. 4a). The purpose of this is to highlight the relationship between the higher β factors and the central axial part of the North Viking Graben, leading northwards into the Møre Basin, and also to show the lower values of β factor away from the axis towards the basin flanks. While these relationships are apparent in standard map form,

they are visually reinforced when displayed on a framework of contemporary structure.

Late Jurassic synrift (155 Ma)

Restoration to the Late Jurassic concludes the backstripping sequence. Figure 6c shows a map of backstripped Late Jurassic synrift palaeobathymetry (at 155 Ma) for the North Viking Graben. This map has been produced by backstripping a further 15 myr from the Base Cretaceous stage of Figure 6b. Figure 7c shows an illuminated 3D perspective display of the same map. Figure 8c shows a cross-section extracted from the model results at this stage.

It should be remembered that the Late Jurassic horizon used for this restoration is not a mapped seismic horizon; it has been interpolated to approximate the top of the Heather Formation, at 50% of the present-day Upper Jurassic thickness. Nevertheless, the map (Fig. 6c), perspective display (Fig. 7c) and cross-section (Fig. 8c) capture nicely the concept of the Late Jurassic synrift archipelago (grey shading on maps) and, in the absence of a reliable regional Top Heather/synrift seismic pick, the interpolated horizon allows us to extend the backstripping beyond the Base Cretaceous to produce a map of the predicted synrift bathymetry and topography.

In this synrift restoration the emergent islands are not isolated from each other, as they are at the Base Cretaceous, instead they take the form of elongate island chains related directly to the Late Jurassic fault system within the North Viking Graben. The morphology of the synrift North Viking Graben is often compared in discussion to the active extensional fault system defining the island and peninsular morphology of the present-day central Aegean Sea, and the adjacent eastern coast of Greece and western coast of Turkey (e.g. Roberts & Jackson 1991; Westaway 1991; Ring *et al.* 2011). To the best of our knowledge, Figures 6c and 7c are the first published maps from a fully quantitative 3D-model to illustrate the details of such a fault-controlled morphology within the North Viking Graben.

The predicted topographical emergence of the islands is the result of synrift footwall uplift (Jackson & McKenzie 1983; Stein & Barrientos 1985). All of the islands are emergent footwalls, bounded by normal faults. The width of the islands is controlled primarily by fault-block width (i.e. the distance between faults), and the height of the islands is controlled primarily by fault displacement (Barr 1987, 1991; Yielding 1990; Yielding & Roberts 1992). Maximum predicted emergence is *c.* 1 km on the Margarita Spur in the north of the area. On the major fault-block structures of Gullfaks, Visund and Magnus, it is *c.* 600–800 m, on Snorre it is *c.* 400–500 m and on Statfjord it is <200 m. Although significant, these predictions of footwall uplift are less than those derived for the same structures by forward modelling (e.g. Marsden *et al.* 1990; Yielding 1990; Yielding & Roberts 1992; Roberts *et al.* 1993a; Berger & Roberts 1999). This is because the backstripping results (Figs 6c, 7c and 8c) are based on restoration of the present-day eroded morphology of these faults blocks, rather than on their initial pre-erosion geometry. To each of the predictions of emergence within the synrift restoration can be added the thickness of the missing section at the crest of each fault block, which in many cases is significant (e.g. Roberts & Yielding 1991; Yielding & Roberts 1992; Yielding *et al.* 1992; Berger & Roberts 1999).

The structural-stratigraphic consequences of footwall uplift leading to erosion of the fault-block crests are two-fold. On the dip slopes of some of the major fault blocks, notably Magnus and Snorre, Upper Jurassic synrift sandstones are present (e.g. Young 1992; Yielding & Roberts 1992; Dahl & Solli 1993). On the footwall crests themselves, and in the adjacent hanging walls, major gravity-driven degradational slide complexes are commonly present (Underhill *et al.* 1997; Berger & Roberts 1999; Hesthammer *et al.* 1999; McLeod & Underhill 1999; Welbon *et al.* 2007). In the

hanging wall of the Visund structure, related synrift conglomerates have also been found within the Draupne Formation (Færseth *et al.* 1995). On the Visund footwall, a dip-slope near-shore environment can be identified in well 34/6-1S (Fig. 6d) where the Heather Formation displays a poorly developed shoreface signature (ConocoPhillips internal study as operator for this well).

Away from the focus on the main Late Jurassic archipelago, the backstripping once more predicts significant water depths within some of the major half-graben structures (Fig. 6c). In the hanging walls (east) of Snorre, Visund and Gullfaks, bathymetry is locally mapped at >1000 m, while further to the north, approaching the Møre Basin, the predicted bathymetry in places exceeds 1500 m. These are similar bathymetric predictions to those seen within the Base Cretaceous restoration (Fig. 6b).

When viewed in a forward time sequence, Figures 6, 7 and 8c–a show how the fault-block morphology that developed during the Late Jurassic persisted with a seafloor expression through until the end of the Early Cretaceous. During the Early Cretaceous, post-rift thermal subsidence drowned most of the emergent fault-block crests below sea level before their relief could be fully removed by erosion/degradation, while sediment deposition was insufficient to fill the seabed relief completely until into the Late Cretaceous.

Summary and conclusions

The post-rift history of the North Viking Graben has been backstripped in 3D, producing a sequence of palaeobathymetric maps which culminates with a Late Jurassic synrift restoration at 155 Ma. The backstripping model has taken into account the three main processes which drive post-rift basin subsidence and development, notably: (i) thermal subsidence; (ii) flexural-isostatic loading; and (iii) sediment compaction. The palaeobathymetric maps have been produced without requiring *a priori* assumptions about water depth as input to the backstripping, and thus the results can and have been validated by calibration against available well and seismic data.

Before backstripping was performed, the Norwegian Trench, within the map of present-day seabed, was filled in and smoothed (Fig. 1c–e) in order to remove related decompaction artefacts from the subsequent backstripped maps.

Palaeobathymetric restorations at the top and base of the Paleocene have taken into account transient dynamic uplift, believed to have been related to the Iceland Plume (Fig. 5); 350 m of uplift is accommodated at the Top Cretaceous–Base Tertiary (65 Ma) and 300 m of uplift is accommodated at the Top Balder (54 Ma).

At the top of the Lower Cretaceous (98.9 Ma) very localized fault-block topography, inherited from the Late Jurassic rift, is predicted to have remained emergent within the basin (Gullfaks and Margarita Spur). At the Base Cretaceous (140 Ma), numerous isolated emergent footwall islands are predicted to have been present, and at the Late Jurassic synrift stage (155 Ma) these islands take the form of elongate island chains along the footwalls of all of the major faults. This is the Jurassic archipelago. The islands were the product of synrift footwall uplift. The footwall emergence predicted by each of these maps calibrates well against available well data and published stratigraphic information. Many examples of calibration have been presented above.

While the backstripping model is believed to calibrate well against known stratigraphic information, it is accepted that there will inevitably be local areas within the maps which do not match precisely the details of the known stratigraphy. This is because the backstripping model has been set up as a regional model with a uniform set of parameters assigned to the whole model. Reasons which could contribute to local inaccuracies might include uncertainties in: seismic interpretation and depth conversion;

extrapolation downwards to produce the top basement horizon; local age of fault movement; accuracy of the map of β factor; flexural-isostatic properties; and lithological properties. Notwithstanding the possibilities that local inaccuracies may be identified, we believe that at the regional scale the model works very well and has consequently been used over several years by ConocoPhillips as a framework for hydrocarbon exploration purposes. In this context, the palaeobathymetry/palaeotopography maps have been used successfully to explain and predict gross depositional environments (GDEs) within the Upper Jurassic, identifying the likely locations of synrift sandstones derived from the eroded footwall blocks, in a similar manner to the earlier work illustrated in Ohm *et al.* (2006).

The results presented here from the backstripping model are only those of palaeobathymetry/palaeotopography, defining the contemporary model surface. Within each stage of the backstripping model, however, the remaining subsurface stratigraphy (Table 1) and its associated internal structure is also present (e.g. Fig. 8) and available as a suite of subsurface palaeostructure maps. In the North Viking Graben, these palaeostructure maps have been used by ConocoPhillips to develop regional models of hydrocarbon migration through time and the consequent charging of prospects. The palaeostructure maps are not illustrated here but comparable examples for the Norwegian Atlantic margin were presented by Roberts *et al.* (2009, 2013).

References

Badley, M.E., Egeberg, T. & Nipen, O. 1984. Development of rift basins illustrated by the structural evolution of the Oseberg feature, Block 30/6, offshore Norway. *Journal of the Geological Society, London*, **141**, 639–649, https://doi.org/10.1144/gsjgs.141.4.0639

Badley, M.E., Price, J.D., Rambech Dahl, C. & Agdestein, T. 1988. The structural evolution of the northern Viking Graben and its bearing upon extensional modes of basin formation. *Journal of the Geological Society, London*, **145**, 455–472, https://doi.org/10.1144/gsjgs.145.3.0455

Barr, D. 1987. Lithospheric stretching, detached normal faulting and footwall uplift. *In*: Coward, M.P., Dewey, J.F. & Hancock, P.L. (eds) *Continental Extensional Tectonics*. Geological Society, London, Special Publications, **28**, 75–94, https://doi.org/10.1144/GSL.SP.1987.028.01.07

Barr, D. 1991. Subsidence and sedimentation in semi-starved half-graben: a model based on North Sea data. *In*: Roberts, A.M., Yielding, G. & Freeman, B. (eds) *The Geometry of Normal Faults*. Geological Society, London, Special Publications, **56**, 17–28, https://doi.org/10.1144/GSL.SP.1991.056.01.02

Beach, A., Bird, T. & Gibbs, A.D. 1987. Extensional tectonics and crustal structure: deep seismic reflection data from the northern North Sea Viking Graben. *In*: Coward, M.P., Dewey, J.F. & Hancock, P.L. (eds) *Continental Extensional Tectonics*. Geological Society, London, Special Publications, **28**, 467–476, https://doi.org/10.1144/GSL.SP.1987.028.01.29

Berger, M. & Roberts, A.M. 1999. The Zeta Structure: a footwall degradation complex formed by gravity sliding on the western margin of the Tampen Spur, Northern North Sea. *In*: Fleet, A. & Boldy, S.A.R. (eds) *Petroleum Geology of Northwest Europe: Proceedings of the 5th Conference*. Geological Society, London, 107–116, https://doi.org/10.1144/0050107

Bertram, G.T. & Milton, N.J. 1988. Reconstructing basin evolution from sedimentary thickness; the importance of palaeobathymetry control, with reference to the North Sea. *Basin Research*, **1**, 247–257, https://doi.org/10.1111/j.1365-2117.1988.tb00020.x

Christiansson, P., Faleide, J.I. & Berge, A.M. 2000. Crustal structure in the northern North Sea: an integrated geophysical study. *In*: Nøttvedt, A. (ed) *Dynamics of the Norwegian Margin*. Geological Society, London, Special Publications, **167**, 15–40, https://doi.org/10.1144/GSL.SP.2000.167.01.01

Dahl, N. & Solli, T. 1993. The structural evolution of the Snorre Field and surrounding areas. *In*: Parker, J.R. (ed) *Petroleum Geology of Northwest Europe. Proceedings of the 4th Conference*. Geological Society, London, 1159–1166, https://doi.org/10.1144/0041159

Dawers, N.H., Berge, A.M., Häger, K.O., Puidefabregas, C. & Underhill, J.R. 1999. Controls on Late Jurassic, subtle sand distribution in the Tampen Spur area, Northern North Sea. *In*: Fleet, A. & Boldy, S.A.R. (eds) *Petroleum Geology of Northwest Europe: Proceedings of the 5th Conference*. Geological Society, London, 107–116, https://doi.org/10.1144/0050827

Eynon, G. 1981. Basin development and sedimentation in the Middle Jurassic of the northern North Sea. *In*: Illing, L.V. & Hobson, G.D. (eds) *Petroleum Geology of the Continental Shelf of North-West Europe*. Heyden & Son, London, 196–204.

Færseth, R.B. 1996. Interaction of Permo-Triassic and Jurassic extensional fault-blocks during the development of the northern North Sea. *Journal of the Geological Society, London*, **153**, 931–944, https://doi.org/10.1144/gsjgs.153.6.0931

Færseth, R.B., Sjøblom, T.S., Steel, R.J., Liljedahl, T., Sauar, B.E. & Tjelland, T. 1995. Tectonic controls on Bathonian–Volgian syn-rift successions on the Visund fault block, northern North Sea. *In*: Steel, R.J., Felt, V., Johannssessen, E. & Mathieu, C. (eds) *Sequence Stratigraphy of the North-West European margin*. Norwegian Petroleum Society, Special Publications, **5**, 325–346.

Fazlikhani, H., Fossen, H., Gawthorpe, R.L., Faleide, J.I. & Bell, R.E. 2017. Basement structure and its influence on the structural configuration of the northern North Sea rift. *Tectonics*, **36**, 1151–1177, https://doi.org/10.1002/2017TC004514

Fossen, H. & Hesthammer, J. 1998. Structural geology of the Gullfaks Field, northern North Sea. *In*: Coward, M.P., Daltaban, T.S. & Johnson, H. (eds) *Structural Geology in Reservoir Characterization*. Geological Society, London, Special Publications, **127**, 231–261, https://doi.org/10.1144/GSL.SP.1998.127.01.16

Fossen, H., Fazlikhani, H., Faleide, J.I., Ksienzyk, A.K. & Dunlap, W.J. 2017. Post-Caledonian extension in the West Norway–northern North Sea region: the role of structural inheritance. *In*: Childs, C., Holdsworth, R.E., Jackson, C.A.-L., Manzocchi, T., Walsh, J.J. & Yielding, G. (eds) *The Geometry and Growth of Normal Faults*. Geological Society, London, Special Publications, **439**, 465–486, https://doi.org/10.1144/SP439.6

Fraser, S.I., Robinson, A.M. *et al.* 2003. Upper Jurassic. *In*: Evans, D., Graham, C., Armour, A. & Bathurst, P. (eds) *The Millennium Atlas: Petroleum Geology of the Central and Northern North Sea*. Geological Society, London, 157–189.

Gabrielsen, R.H., Kyrkjebø, R., Faleide, J.I., Fjeldskaar, W. & Kjennerud, T. 2001. The Cretaceous post-rift basin configuration of the northern North Sea. *Petroleum Geoscience*, **7**, 137–154, https://doi.org/10.1144/petgeo.7.2.137

Giltner, J.P. 1987. Application of extensional models to the Northern Viking Graben. *Norsk Geologisk Tidsskrift*, **67**, 339–352.

Haq, B., Hardenbol, J. & Vail, P.R. 1987. Chronology of fluctuating sea level since the Triassic (250 million years to present). *Science*, **25**, 1156–1167, https://doi.org/10.1126/science.235.4793.1156

Hesthammer, J., Jourdan, C.A., Nielsen, P.E., Ekern, T.E. & Gibbons, K.A. 1999. A tectonostratigraphic framework for the Statfjord field, northern North Sea. *Petroleum Geoscience*, **5**, 241–256, https://doi.org/10.1144/petgeo.5.3.241

Hollander, N.B. 1987. Snorre. *In*: Spencer, A.M. (ed.) *Geology of the Norwegian Oil and Gas Fields*. Graham & Trotman, London, 307–318.

Jackson, J.A. & McKenzie, D.P. 1983. The geometrical evolution of normal fault systems. *Journal of Structural Geology*, **5**, 471–482, https://doi.org/10.1016/0191-8141(83)90053-6

Jarvis, G.T. & McKenzie, D.P. 1980. Sedimentary basin formation with finite extension rates. *Earth and Planetary Science Letters*, **48**, 42–52, https://doi.org/10.1016/0012-821X(80)90168-5

Joy, A.M. 1992. Right place, wrong time: anomalous post-rift subsidence in sedimentary basins around the North Atlantic Ocean. *In*: Storey, B.C., Alabaster, T. & Pankhurst, R.J. (eds) *Magmatism and the Causes of Continental Break-up*. Geological Society, London, Special Publications, **68**, 387–393, https://doi.org/10.1144/GSL.SP.1992.068.01.24

Joy, A.M. 1993. Comments on the pattern of post-rift subsidence in the Central and Northern North Sea Basin. *In*: Williams, G.D. & Dobb, A. (eds) *Tectonics and Seismic Sequence Stratigraphy*. Geological Society, London, Special Publications, **71**, 113–140, https://doi.org/10.1144/GSL.SP.1993.071.01.06

Kjennerud, T. & Gilmore, G.K. 2003. Integrated Palaeogene palaeobathymetry of the northern North Sea. *Petroleum Geoscience*, **9**, 125–132, https://doi.org/10.1144/1354-079302-510

Kjennerud, T. & Sylta, Ø. 2001. Application of quantitative palaeobathymetry in basin modelling, with reference to the northern North Sea. *Petroleum Geoscience*, **7**, 331–341, https://doi.org/10.1144/petgeo.7.4.331

Klemperer, S. & Hobbs, R. 1991. *The BIRPS Atlas: Deep Seismic Reflection Profiles Around the British Isles*. Cambridge University Press, Cambridge.

Kusznir, N.J., Marsden, G. & Egan, S. 1991. A flexural-cantilever simple-shear/pure-shear model of continental lithosphere extension: applications to the Jeanne d'Arc Basin, Grand Banks and Viking Graben, North Sea. *In*: Roberts, A.M., Yielding, G. & Freeman, B. (eds) *The Geometry of Normal Faults*. Geological Society, London, Special Publications, **56**, 41–60, https://doi.org/10.1144/GSL.SP.1991.056.01.04

Kusznir, N.J., Roberts, A.M. & Morley, C. 1995. Forward and reverse modelling of rift basin formation. *In*: Lambiase, J. (ed) *Hydrocarbon Habitat in Rift Basins*. Geological Society, London, Special Publications, **80**, 33–56, https://doi.org/10.1144/GSL.SP.1995.080.01.02

Kusznir, N.J., Hunsdale, R. & Roberts, A.M. 2004. Timing of depth-dependent stretching on the S. Lofoten rifted margin Mid-Norway: pre-breakup or post-

breakup? *Basin Research*, **16**, 279–296, https://doi.org/10.1111/j.1365-2117.2004.00233.x

Kusznir, N.J., Hunsdale R., Roberts, A.M. & iSIMM Team. 2005, Timing and magnitude of depth-dependent lithosphere stretching on the southern Lofoten and northern Vøring continental margins offshore mid-Norway: implications for subsidence and hydrocarbon maturation at volcanic rifted margins. *In*: Doré, A.G. & Vining, B.A. (eds) *Petroleum Geology: North-West Europe and Global Perspectives – Proceedings of the 6th Petroleum Geology Conference*. Geological Society, London, 767–783, https://doi.org/10.1144/0060767

Livera, S.E. & Gdula, J.E. 1990. Brent Oil Field. *In*: Beaumont, E.A. & Foster, N.H. (eds) *Structural Traps II – Traps Associated with Tectonic Faulting*. Treatise of Petroleum Geology Atlas of Oil and Gas Fields. American Association of Petroleum Geologists, Tulsa, OK, 21–63.

Maclennan, J. & Lovell, B. 2002. Control of regional sea level by surface uplift and subsidence caused by magmatic underplating of Earth's crust. *Geology*, **30**, 675–678, https://doi.org/10.1130/0091-7613(2002)030<0675:CORSLB>2.0.CO;2

Marsden, G., Yielding, G., Roberts, A.M. & Kusznir, N.J. 1990. Application of a flexural cantilever simple-shear/pure-shear model of continental lithosphere extension to the formation of the North Sea. *In*: Blundell, D.J. & Gibbs, A.D. (eds) *Tectonic Evolution of the North Sea Rifts*. Oxford University Press, New York, 241–261.

McKenzie, D.P. 1978. Some remarks on the development of sedimentary basins. *Earth and Planetary Science Letters*, **40**, 25–32, https://doi.org/10.1016/0012-821X(78)90071-7

McLeod, A.E. & Underhill, J.R. 1999. Processes and products of footwall degradation, northern Brent Field, northern North Sea. *In*: Fleet, A. & Boldy, S.A.R. (eds) *Petroleum Geology of Northwest Europe: Proceedings of the 5th Conference*. Geological Society, London, 91–106, https://doi.org/10.1144/0050091

Milton, N.J., Bertram, G.T. & Vann, I.R. 1990. Early Palaeogene tectonics and sedimentation in the Central North Sea. *In*: Hardman, R.F.P. & Brooks, J. (eds) *Tectonic Events Responsible for Britain's Oil and Gas Reserves*. Geological Society, London, Special Publications, **55**, 339–351, https://doi.org/10.1144/GSL.SP.1990.055.01.16

Nadin, P.A. & Kusznir, N.J. 1995. Palaeocene uplift and Eocene subsidence in the northern North Sea Basin from 2D forward and reverse stratigraphic modelling. *Journal of the Geological Society, London*, **152**, 833–848, https://doi.org/10.1144/gsjgs.152.5.0833

Nadin, P.A., Kusznir, N.J. & Toth, J. 1995. Transient regional uplift in the Early Tertiary of the northern North Sea and the development of the Iceland Plume. *Journal of the Geological Society, London*, **152**, 953–958, https://doi.org/10.1144/GSL.JGS.1995.152.01.12

Nadin, P.A., Kusznir, N.J. & Cheadle, M.J. 1997. Early Tertiary plume uplift in the North Sea and Faeroe–Shetland Basin. *Earth and Planetary Science Letters*, **148**, 109–127, https://doi.org/10.1016/S0012-821X(97)00035-6

Nøttvedt, A. (ed.). 2000. *Dynamics of the Norwegian Margin*. Geological Society, London, Special Publications, **167**, https://doi.org/10.1144/GSL.SP.2000.167.01.20

NPD. 2018. *NPD Fact Pages. Norwegian Petroleum Directorate Data Archive*. Norwegian Petroleum Directorate, Stavanger, Norway, http://factpages.npd.no/factpages/

Odinsen, T., Christiansson, P., Gabrielsen, R.H., Faleide, J.I. & Berge, A.M. 2000*a*. The geometries and deep structure of the northern North Sea rift system. *In*: Nøttvedt, A. (ed.) *Dynamics of the Norwegian Margin*. Geological Society, London, Special Publications, **167**, 41–57, https://doi.org/10.1144/GSL.SP.2000.167.01.03

Odinsen, T., Reemst, P., Van Der Beek, P., Faleide, J.I. & Gabrielsen, R.H. 2000*b*. Permo-Triassic and Jurassic extension in the northern North Sea: results from tectonostratigraphic forward modelling. *In*: Nøttvedt, A. (ed) *Dynamics of the Norwegian Margin*. Geological Society, London, Special Publications, **167**, 83–103, https://doi.org/10.1144/GSL.SP.2000.167.01.05

Ohm, S.E., Beeley, H., Karlsen, D.A., Hall, P.B. & Foss, A. 2006. An atypical early mature oil in Block 35/1, Norwegian North Sea – hypersaline, carbonate Jurassic environment? *Petroleum Geoscience*, **12**, 157–174, https://doi.org/10.1144/1354-079305-685

Rattey, R.P. & Hayward, A.B. 1993. Sequence stratigraphy of a failed rift system: the Middle Jurassic to Early Cretaceous basin evolution of the Central and Northern North Sea. *In*: Parker, J.R. (ed) *Petroleum Geology of Northwest Europe. Proceedings of the 4th Conference*. Geological Society, London, 215–249, https://doi.org/10.1144/0040215

Ravnås, R., Nøttvedt, A., Steel, R.J. & Windelstad, J. 2000. Syn-rift sedimentary architectures in the Northern North Sea. *In*: Nøttvedt, A. (ed) *Dynamics of the Norwegian Margin*. Geological Society, London, Special Publications, **167**, 133–177, https://doi.org/10.1144/GSL.SP.2000.167.01.07

Ring, U., Glodny, J., Will, T.M. & Thomson, S. 2011. Normal faulting on Sifnos and the South Cycladic Detachment System, Aegean Sea, Greece. *Journal of the Geological Society, London*, **168**, 751–768, https://doi.org/10.1144/0016-76492010-064

Roberts, S. & Jackson, J.A. 1991. Active normal faulting in Central Greece: an overview. *In*: Roberts, A.M., Yielding, G. & Freeman, B. (eds) *The Geometry of Normal Faults*. Geological Society, London, Special Publications, **56**, 125–142, https://doi.org/10.1144/GSL.SP.1991.056.01.09

Roberts, A.M. & Yielding, G. 1991. Deformation around basin-margin faults in the North Sea/mid-Norway rift. *In*: Roberts, A.M., Yielding, G. & Freeman, B. (eds) *The Geometry of Normal Faults*. Geological Society, London, Special Publications, **56**, 61–78, https://doi.org/10.1144/GSL.SP.1991.056.01.05

Roberts, A.M., Yielding, G. & Badley, M.E. 1993*a*. Tectonic and bathymetric controls on stratigraphic sequences within evolving half-graben. *In*: Williams, G.D. & Dobb, A. (eds) *Tectonics and Seismic Sequence Stratigraphy*. Geological Society, London, Special Publications, **71**, 87–121, https://doi.org/10.1144/GSL.SP.1993.071.01.05

Roberts, A.M., Yielding, G., Kusznir, N.J., Walker, I. & Dorn-Lopez, D. 1993*b*. Mesozoic extension in the North Sea: constraints from flexural backstripping, forward modelling and fault populations. *In*: Parker, J.R. (ed) *Petroleum Geology of Northwest Europe: Proceedings of the 4th Conference*. Geological Society, London, 1123–1136, https://doi.org/10.1144/0041123

Roberts, A.M., Yielding, G., Kusznir, N.J., Walker, I. & Dorn-Lopez, D. 1995. Quantitative analysis of Triassic extension in the Northern Viking Graben. *Journal of the Geological Society, London*, **152**, 15–26, https://doi.org/10.1144/gsjgs.152.1.0015

Roberts, A.M., Lundin, E.R. & Kusznir, N.J. 1997. Subsidence of the Vøring Basin and the influence of the Atlantic continental margin. *Journal of the Geological Society, London*, **154**, 551–557, https://doi.org/10.1144/gsjgs.154.3.0551

Roberts, A.M., Kusznir, N.J., Yielding, G. & Styles, P. 1998. 2D flexural backstripping of extensional basins; the need for a sideways glance. *Petroleum Geoscience*, **4**, 327–338, https://doi.org/10.1144/petgeo.4.4.327

Roberts, A.M., Corfield, R.I., Kusznir, N.J., Matthews, S.J., Kåre-Hansen, E. & Hooper, R.J. 2009. Mapping palaeostructure and palaeobathymetry along the Norwegian Atlantic continental margin: Møre and Vøring basins. *Petroleum Geoscience*, **15**, 27–43, https://doi.org/10.1144/1354-079309-804

Roberts, A.M., Kusznir, N.J., Corfield, R.I., Thompson, M. & Woodfine, R. 2013. Integrated tectonic basin modelling as an aid to understanding deep-water rifted continental margin structure and location. *Petroleum Geoscience*, **19**, 65–88, https://doi.org/10.1144/petgeo2011-046

Roberts, A.M., Alvey, A.D. & Kusznir, N.J. 2018. Crustal structure and heat-flow history in the UK Rockall Basin, derived from backstripping and gravity-inversion analysis. *Petroleum Geoscience*. First published online 15 May 15, 2018, https://doi.org/10.1144/petgeo2017-063

Sclater, J.G. & Christie, P.A.F. 1980. Continental stretching: an explanation of the post mid-Cretaceous subsidence of the Central North Sea Basin. *Journal of Geophysical Research*, **85**, 3711–3739, https://doi.org/10.1029/JB085iB07p03711

Shepherd, M. 1991. The Magnus Field, Block 211/7a, 12a, UK North Sea. *In*: Abbotts, I.L. (ed.) *United Kingdom Oil and Gas Fields: 25 Years Commemorative Volume*. Geological Society, London, Memoirs, **14**, 153–157, https://doi.org/10.1144/GSL.MEM.1991.014.01.19

Smith, W.H.F. & Sandwell, D.T. 1997. Global seafloor topography from satellite altimetry and ship depth soundings. *Science*, **277**, 1957–1196, https://doi.org/10.1126/science.277.5334.1956; updates, http://topex.ucsd.edu/marine_topo/

Statoil. 2013. Press release: *Statoil makes oil discovery at Gullfaks in North Sea*, https://www.offshore-technology.com/uncategorised/newsstatoil-oil-discovery-gullfaks-field-north-sea/

Statoil. 2015*a*. Press release: *Plan for development in the Gullfaks area submitted*, https://www.statoil.com/en/news/2015/06/30/article.html

Statoil. 2015*b*. Press release: *Statoil to convert Gullfaks wells for Shetland/Lista development*, https://www.offshore-mag.com/articles/2015/06/statoil-to-convert-gullfaks-wells-for-shetland-lista-development.html

Steel, R. & Ryseth, A. 1990. The Triassic–early Jurassic succession in the northern North Sea: megasequence stratigraphy and intra-Triassic tectonics. *In*: Hardman, R.F.P. & Brooks, J. (eds) *Tectonic Events Responsible for Britain's Oil and Gas Reserves*. Geological Society, London, Special Publications, **55**, 139–168, https://doi.org/10.1144/GSL.SP.1990.055.01.07

Stein, R.S. & Barrientos, S.E. 1985. Planar high-angle faulting in the basin and range: Geodetic analysis of the 1983 Borah Peak, Idaho, earthquake. *Journal of Geophysical Research*, **90**, 11 355–11 366, https://doi.org/10.1029/JB090iB13p11355

Steinberg, J., Roberts, A.M., Kusznir, N.J., Schafer, K. & Karcz, Z. 2018. Crustal structure and post-rift evolution of the Levant Basin. *Marine and Petroleum Geology*, **96**, 522–543, https://doi.org/10.1016/j.marpetgeo.2018.05.006

Ter Voorde, M., Færseth, R.B., Gabrielsen, R.H. & Cloetingh, S.A.P.L. 2000. Repeated lithosphere extension in the northern Viking Graben: a coupled or decoupled rheology? *In*: Nøttvedt, A. (ed) *Dynamics of the Norwegian Margin*. Geological Society, London, Special Publications, **167**, 59–81, https://doi.org/10.1144/GSL.SP.2000.167.01.04

Underhill, J.R. & Partington, M.A. 1993*a*. Jurassic thermal doming and deflation in the North Sea: implications of the sequence stratigraphic evidence. *In*: Parker, J.R. (ed) *Petroleum Geology of Northwest Europe: Proceedings of the 4th Conference*. Geological Society, London, 337–345, https://doi.org/10.1144/0040337

Underhill, J.R. & Partington, M.A. 1993*b*. Use of genetic sequence stratigraphy in determining a regional tectonic control on the 'Mid Cimmerian Unconformity': implications for North Sea basin development. *In*: Weimer, P. & Posamentier, H.W. (eds) *Siliciclastic Sequence Stratigraphy*. AAPG Memoirs, **58**, 449–483.

Underhill, J.R., Sawyer, M.J., Hodgson, P., Shallcross, M.D. & Gawthorpe, R.L. 1997. Implications of fault scarp degradation for Brent Group prospectivity, Ninian Field, Northern North Sea. *AAPG Bulletin*, **81**, 999–1022.

Welbon, A.I.F., Brockbank, P.J., Brunsden, D. & Olsen, T.S. 2007. Characterizing and producing from reservoirs in landslides: challenges and opportunities. *In*: Jolley, S.J., Barr, D., Walsh, J.J. & Knipe, R.J. (eds) *Structurally Complex Reservoirs*. Geological Society, London, Special Publications, **292**, 49–74, https://doi.org/10.1144/SP292.3

Wennberg, O.P., Wall, B.G., Saether, E., Jounund, S., Rozhko, A. & Naumann, M. 2018. Fractures in chalks and marls of the Shetland Group in the Gullfaks Field, North Sea. Extended abstract presented at the 80th EAGE Conference and Exhibition, 11–14 June 2018, Copenhagen, Denmark, https://doi.org/10.3997/2214-4609.201801488

Westaway, R. 1991. Continental extension on sets of parallel faults: observational evidence and theoretical models. *In*: Roberts, A.M., Yielding, G. & Freeman, B. (eds) *The Geometry of Normal Faults*. Geological Society, London, Special Publications, **56**, 143–169, https://doi.org/10.1144/GSL.SP.1991.056.01.10

White, N.J. 1990. Does the uniform stretching model work in the North Sea? *In*: Blundell, D.J. & Gibbs, A.D. (eds) *Tectonic Evolution of the North Sea Rifts*. Oxford University Press, New York, 217–239.

White, R.S. 1999. The lithosphere under stress. *Philosophical Transactions of the Royal Society A: Mathematical, Physical and Engineering Sciences*, **357**, 901–915, https://doi.org/10.1098/rsta.1999.0357

Yielding, G. 1990. Footwall uplift associated with Late Jurassic normal faulting in the northern North Sea. *Journal of the Geological Society, London*, **147**, 219–222, https://doi.org/10.1144/gsjgs.147.2.0219

Yielding, G. & Roberts, A.M. 1992. Footwall uplift during normal faulting – implications for structural geometries in the North Sea. *In*: Larsen, R.M., Brekke, H., Larsen, B.T. & Talleras, E. (eds) *Structural and Tectonic Modelling and its Application to Petroleum Geology*. Norwegian Petroleum Society, Special Publications, **1**, 289–304.

Yielding, G., Badley, M.E. & Roberts, A.M. 1992. The structural evolution of the Brent Province. *In*: Morton, A.C., Haszeldine, R.S., Giles, M.R. & Brown, S. (eds) *Geology of the Brent Group*. Geological Society, London, Special Publications, **61**, 27–43, https://doi.org/10.1144/GSL.SP.1992.061.01.04

Young, R. 1992. Restoration of a regional profile across the Magnus Field in the northern North Sea. *In*: Larsen, R.M., Brekke, H., Larsen, B.T. & Talleras, E. (eds) *Structural and Tectonic Modelling and its Application to Petroleum Geology*. Norwegian Petroleum Society, Special Publications, **1**, 221–229.

Zanella, E. & Coward, M.P. 2003. Structural framework. *In*: Evans, D., Graham, C., Armour, A. & Bathurst, P. (eds) *The Millennium Atlas: Petroleum Geology of the Central and Northern North Sea*. Geological Society, London, 45–59.